Observation of parity nonconservation in atoms

L. M. Barkov, M. S. Zolotorev, and I. B. Khriplovich

Institute of Nuclear Physics, Siberian Branch of the Academy of Sciences of the USSR, Novosibirsk
Usp. Fiz. Nauk **132**, 409–442 (November 1980)

This article examines new directions in physical research: the study of the weak interactions of elementary particles using optical methods. Calculations of the effects of parity nonconservation in heavy atoms are discussed and an experiment, in which parity nonconservation in atoms and the weak interaction of electrons and nucleons arising from neutral currents were first observed, is described.

PACS numbers: 35.10.Hn, 13.60.Hb

CONTENTS

1. INTRODUCTION

In recent years, a new trend has appeared in physics research: the study of the weak interaction of elementary particles using atomic spectroscopy. Not too long ago, many Physicists thought of this research as no more than a realm of science fiction, while attempts to discuss revelent experiments only gave rise to cheerful gaiety among the audience. Nevertheless, beginning in 1974, weak interactions in atomic physics became not only a subject of theoretical, but also of persistent experimental, investigations. The first positive result was obtained at the beginning of 1978. It was discovered at the Institute of Nuclear Physics, Siberian Branch of the Academy of Sciences of the USSR in Novosibirsk, that atomic bismuth vapor is optically active, i.e, the vapor rotates the plane of polarization of light passing through it.[1,2] Optical activity is one of the most striking demonstrations of parity nonconservation, the absence of symmetry between right and left: the plane of polarization of light prefers, for instance, left-handed rotation to right-handed rotation. Here, parity violation was first manifested as a coherent macroscopic phenomenon. From the point of view of modern ideas, the observed parity violation can be explained by the existence of a weak interaction between electrons and nucleons, caused by the so-called neutral currents. Such an interaction is predicted by models that unify electromagnetic and weak interactions of elementary particles. It is difficult to overestimate the importance of creating a unified theory of electromagnetic and weak interactions that is not only internally consistent, but also experimentally verified. The experimentally observed magnitude of this effect agrees quantitatively with the predictions of one of these models, proposed by Weinberg[3] and Salam.[4]

Parity nonconserving weak interaction of electrons with nucleons was later also observed in a completely different type of experiment, carried out with the two-mile linear accelerator at Stanford (SLAC), involving deep inelastic scattering of longitudinally polarized electrons by deuterons and protons.[5]

The discovery of a new form of parity nonconservation by weak interactions of electrons with nucleons is an example of how one branch of physics (we are talking about atomic spectroscopy), which has long since become classical, again appears at the frontiers of our knowledge of nature. This history once again clearly demonstrates the internal unity of physics. It has demonstrated once again that the days of "room-sized" experiments in research on the fundamental properties of matter have by no means ended.

In this article, we shall discuss the investigation of parity nonconservation in atomic processes, primarily, in the usual $M1$-transitions in heavy atoms. Naturally, investigations in which the authors participated will be described in greatest detail.

2. CHARGED AND NEUTRAL CURRENTS OF WEAK INTERACTIONS

Such well-known weak processes as neutron β-decay

$$n \to p e^- \bar{\nu}_e,$$

 0038-5670/80/110713-19$01.10

or transformation of a high-energy neutrino in the presence of a nucleus into a muon involve a change in the electric charge of strongly interacting particles, hadrons. The matrix elements of these processes can be written as a product of the hadronic vector current by a leptonic vector current: e, ν_e, μ, and ν_μ. Due to the fact that the charge of the particles entering into each current changes, these currents are referred to as charged. The purely leptonic process of muon decay is also described in terms of the interaction of charged currents:

$$\mu^- \to e^- \bar{\nu}_e \nu_\mu,$$

as well as such purely hadronic processes as nonleptonic decays of hyperons.

Meanwhile, the known conservation laws do not forbid weak interactions of hadrons and leptons that do not involve charge transfer, for example, elastic scattering of a neutrino, electron, or muon by a nucleon. Currents, in terms of which the amplitudes of such reactions are expressed, are referred to as neutral. Neutral currents would also lead to purely leptonic processes, such as the elastic scattering of an electron by an electron or a muon neutrino by an electron. Together with charged currents, it would also contribute to the scattering of the electron neutrino by an electron and to nuclear forces that do not conserve parity. The relevance of neutral currents to atomic experiments is examined in greater detail, for example, in Ref. 6.

The possibility of the existence of neutral currents has been discussed for a long time. However, special interest has arisen in neutral currents in connection with the fact that their existence was predicted by unified theories of electromagnetic and weak interactions (see, for example, Ref. 7).

Neutral currents were discovered experimentally with the accelerators in CERN[8,9] and in Batavia (Illinois).[10] In these experiments, the scattering of muonic neutrinos and antineutrinos by nucleons and electrons, not involving the transformation of the neutrinos into muons, was observed.

However, until recently, there were no experimental data on weak interaction of electrons with nucleons caused by neutral currents. The point is that in such processes it is extremely difficult to separate out the contribution of the weak interaction against the background of the electromagnetic interaction, which is much stronger. One possibility here is the investigation of fine atomic effects. Another possibility is an increase in the energy, since as energy increases the weak interaction, in contrast with the electromagnetic interaction, increases at least to energies of several tens of gigaelectron-volts in the center-of-mass system of the colliding particles (see, for example, Ref. 11). At these energies, its contribution to the scattering cross section is comparable to that of the electromagnetic interaction. With existing accelerators and in atomic physics, we can only hope to discover qualitatively new phenomena caused by the weak interaction. Parity nonconservation, which can be ascribed only to the weak interaction, is such a characteristic property.

3. DISCUSSION OF PARITY NONCONSERVATION EFFECTS IN ATOMS

The possible effects of parity nonconservation in atoms, caused by neutral currents, were first discussed by Ya. B. Zel'dovich.[12] An extremely important step was taken by M. B. Bouchiat and C. Bouchiat, who showed[13] that these effects are enhanced in heavy atoms to such an extent that it is possible to observe them in induced strongly forbidden $M1$-transitions.

a) Weak interaction of an electron and a nucleus

The interaction of an electron and a nucleon, which does not conserve spatial parity but is invariant relative to time reversal, in general contains four independent terms[6)] and can be represented in the following form:

$$H=\frac{G}{\sqrt{2}}\Big\{-\bar{u}_e\gamma_\mu\gamma_5 u_e\Big[\varkappa_1\bar{u}_N\gamma_\mu u_N+\frac{\varkappa_3}{2m_p}i\partial_\nu(\bar{u}_N\sigma_{\mu\nu}u_N)\Big]+\Big[\varkappa_2\bar{u}_e\gamma_\mu u_e+\frac{\varkappa_4}{2m}i\partial_\nu(\bar{u}_e\sigma_{\mu\nu}u_e)\Big]\bar{u}_N\gamma_\mu\gamma_5 u_N\Big\}. \tag{1}$$

Here, $G=1.026\cdot10^{-5}/m_p^2$ is the Fermi constant for the weak interaction, u_e and u_N are the four-component Dirac wave functions of the electron and nucleon, m and m_p are the electron and proton mass, γ_μ are the Dirac matrices, $\gamma_5=-i\gamma_0\gamma_1\gamma_2\gamma_3$, and $\sigma_{\mu\nu}=\frac{1}{2}(\gamma_\mu\gamma_\nu-\gamma_\nu\gamma_\mu)$. A system of units for which $\hbar=c=1$ is used. The dimensionless constants $\varkappa_i$ are unknown, and, in essence, the point of the experiments to be discussed is to determine these constants.

We shall present some arguments showing that the terms with the derivatives in (1) can be neglected. It is natural to expect that the "anomalous weak moment" of the electron $\varkappa_4$ arises only a a result of radiative corrections, as in the case of the anomalous magnetic moment, and therefore is very small, $\sim\alpha/2\pi$. The term with $\varkappa_3$ can be dropped since it contains the large mass m_p in the denominator. Dropping terms $\sim m_p^{-1}$ and terms containing $\varkappa_{1,2}$, we arrive at the following expression for the interaction of an electron and a nucleon:

$$H=\frac{G}{\sqrt{2}}(-\varkappa_1\psi^+\psi u_e^+\gamma_5 u_e+\varkappa_2\psi^+\sigma_N\psi u_e^+\alpha u_e). \tag{2}$$

Here, σ_N are the nucleon Pauli matrices, ψ are the nonrelativistic two-component wave functions of the nucleon, and $\alpha=\gamma_0\gamma$. Using formula (2), it is easy to obtain the Hamiltonian describing the interaction of the electron and a nucleus:

$$H=-\frac{G}{\sqrt{2}}(Zq\rho(\mathbf{r})\gamma_5-\Sigma(\mathbf{r})\bar{\alpha}), \tag{3}$$

$$Zq=Z\varkappa_{1p}+(A-Z)\varkappa_{1n}, \tag{3a}$$

$$\Sigma(\mathbf{r})=\varkappa_{2p}\sum\sigma_p(\mathbf{r})+\varkappa_{2n}\sum\sigma_n(\mathbf{r}), \tag{3b}$$

$\rho(\mathbf{r})$ is the nucleon density in the nucleus, normalized to unity, $\sigma_p(\mathbf{r})$ and $\sigma_n(\mathbf{r})$ are the single-particle proton and neutron spin densities. The summation in (3b) extends over all Z protons and $A-Z$ neutrons in the nucleus. The vector $\langle\Sigma(\mathbf{r})\rangle$ is oriented, obviously, along

the nuclear spin i. In contrast to expressions (1) and (2), describing the interaction of the electron and nucleon fields, the Hamiltonian (3) has the usual quantum mechanical meaning: it is an operator acting in the space of the Dirac wave functions of the electron.

In heavy atoms, the second term in (3) is much less than the first term, since, as a result of the pairing of proton and neutron spins in the nucleus,

$$|\Sigma(\mathbf{r})| \sim \varkappa\rho(\mathbf{r}) \ll Zq\rho(\mathbf{r}) \sim Z\varkappa\rho(\mathbf{r}).$$

For this reason, in what follows, we shall discuss primarily the weak interaction that does not depend on the spin of the nucleus. It is useful to write it in nonrelativistic form:

$$H = \frac{G}{\sqrt{2}} \frac{Zq}{2m} [\sigma\mathbf{p}\delta(\mathbf{r}) + \delta(\mathbf{r})\sigma\mathbf{p}]. \tag{4}$$

Here, $\mathbf{p}$ and $\sigma/2$ are the momentum and spin of the electron. In this limit, the nucleus can be considered as a point, so that here the density $\rho(\mathbf{r})$ is replaced by a δ-function.

In the Weinberg–Salem model[3,4]

$$\varkappa_{1p} = \frac{1}{2}(1 - 4\sin^2\theta), \quad \varkappa_{1n} = -\frac{1}{2}, \qquad \varkappa_{2p} = -\varkappa_{2n} = -\frac{1}{2}(1 - 4\sin^2\theta)\cdot 1.25, \tag{5}$$

where θ is an independent parameter of the theory. The predictions of this model with $\sin^2\theta \approx 0.25$ agree well at the present time with all of the experimental data on neutral currents. We note that in this case the constants $\varkappa_{2p,n}$ are numerically small, which leads to the additional suppression of the term that depends on the spin of the nucleus in the Hamiltonian (3).

The interaction being discussed is a pseudoscalar and therefore leads to mixing of atomic states with the same angular momenta, but opposite parity. It is clear from expression (4) that (4) mixes only the electronic $s_{1/2}$- and $p_{1/2}$-states. This assertion is also valid for the total relativistic Hamiltonian (3).

b) Spin ringlet

Let us now consider an illustrative picture that gives a qualitative understanding of how the mixing of levels with opposite parity effects the structure of an atom. Let the $p_{1/2}$ state be mixed into the $s_{1/2}$ state due to the weak interaction. We write the $s_{1/2}$ wave in the usual form

$$\frac{1}{\sqrt{4\pi}} R_0(r)\chi, \tag{6}$$

where $R_0(r)$ is the radial s-state function, while χ is a two-component spinor, describing the spin state of the electron. As far as $p_{1/2}$ is concerned, its wave function also has two components, since the total angular momentum of this state is $j = 1/2$. In addition, it is linear in the spherical harmonic with $l = 1$, i.e., with respect to the unit radius vector $\mathbf{n} = \mathbf{r}/r$. It is easy to see that the wave function that satisfies these requirements

$$\frac{1}{\sqrt{4\pi}} R_1(r)(-\sigma\mathbf{n})\chi \tag{7}$$

corresponds simultaneously to the standard definition of the spherical harmonics and the usual method for adding angular momenta $l = 1$ and $s = 1/2$ to form $j = 1/2$. Choosing the radial function of the p-state as $R_1(r)$, we thereby identify (7) with the wave function of the $p_{1/2}$ state.

The wave function that results from the mixing is as follows:

$$\frac{1}{\sqrt{4\pi}} [R_0(r) - i\eta R_1(r)\sigma\mathbf{n}]\chi. \tag{8}$$

The fact that the mixing coefficient $i\eta$ is imaginary follows from the T-invariance of the weak interaction. Indeed, both terms in (8) must transform in the same way under T-reversal, and this operation involves not only the transformation $\sigma \to -\sigma$ (obviously, the angular momentum, as well as the momentum, changes sign under time reversal), but also requires that the initial and final states be reversed, i.e., Hermitian conjugation of the wave function. It is easy to verify that the phase of the mixing has this property by direct computation of the matrix elements, for example, of the Hamiltonian (4).

The wave function (8) can be rewritten in the form

$$\frac{1}{\sqrt{4\pi}} R_0(r) \exp\left(-i\varphi\frac{\sigma\mathbf{n}}{2}\right)\chi, \tag{9}$$

from which it is evident that the resulting admixture is equivalent to a local rotation of the spinor χ in the initial expression (6) by an angle

$$\varphi(r) = \operatorname{arctg}\frac{2\eta R_1(r)}{R_0(r)} \approx \frac{2\eta R_1(r)}{R_0(r)} \tag{10}$$

around the direction n.

In particular, if in the initial state $s_{1/2}$ the spin is directed along the z axis, then depending on the distance from the origin of coordinates $r = 0$ [we recall that $R_1(0) = 0$] in the xy plane, the spin acquires a projection in this plane, oriented along the tangent to the circle centered at the origin of coordinates. The configuration that arises, as illustrated in Fig. 1, is nothing more than a spin ringlet.[14,15] We note that the symmetry of this ringlet, i.e., right-handed or left-handed, evidently, does not depend on the orientation of the spin at $z = 0$. It is thus not surprising that the unpolarized state of the atom is also characterized by the same ringlet.

The current distribution in such a atom also has a curious form. Together with the usual circulating current, flowing in a plane that is orthogonal to the angular momentum, there is a component that corresponds to the current in a winding wound around a torus.[14] A.S. Kompaneĭts suggested the term anapole for such an electromagnetic field source.

It is entirely natural that the probabilities for the

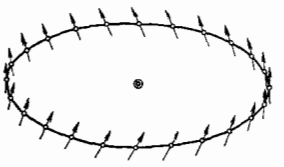

FIG. 1. Spin ringlet.

emission of right- and left-polarized photons by such an atom are different; in other words, the emitted radiation is circularly polarized. This is what indicates the violation of parity conservation in atomic transitions.

c) Simple estimates

Let us now examine, for definiteness, a magnetic dipole transition in an atom. Due to the weak interaction, states with opposite parity are mixed into the upper and lower levels. As a result, the amplitude of the $M1$-transition $A\,(M1)$ acquires an admixture of the $E1$-amplitude $A\,(E1)$. Since the parities of the operators for the $M1$- and E1-transitions are different, the relative signs of the admixtures are different for right- and left-polarized quanta. It can further be shown that due to T-invariance, the $M1$- and $E1$ amplitudes have maximum interference. Thus, the emitted radiation is circularly polarized with a degree of polarization given by

$$P=\frac{W_+-W_-}{W_++W_-}=2\sum_n \eta_n \frac{A_n(E1)}{A(M1)}. \tag{11}$$

The summation in (11) extends over states with opposite parity, which are mixed into the upper and lower levels.

Let us make a simple estimate of the degree of circular polarization in heavy atoms. As first noted in Ref. 13, the mixing coefficient

$$\eta=\frac{\langle H\rangle}{\Delta E}\sim GZ\frac{|\psi(0)|^2}{\Delta E}\frac{p}{m}R \tag{12}$$

[see (3) and (4)] increases more rapidly with nuclear charge Z than Z^3. It is not difficult to understand why this happens.[1)] In the region $r\sim a$, where the nucleus is screened by the rest of the electrons, the potential energy of the external electron is $V\sim -\alpha/r$. And, since the electron is most often located in this particular region, the total energy of the electron is $E\sim -\alpha/a$. On the other hand, for $r\ll a/Z^{1/3}$, screening of the nucleus is not important and the magnitude of the potential energy $V(r)\approx -Z\alpha/r$ is much greater than the total energy. At distances $r\gg a/Z$, the wave function ψ of the external electron is quasiclassical, so that in the interval $a/Z \ll r\ll a/Z^{1/3}$, it may be approximated by

$$\psi(r)\sim\frac{1}{r\sqrt{p(r)}}\sim\frac{1}{r\sqrt[4]{V(r)}}. \tag{13}$$

The coefficient here does not depend on Z, since for $r\sim a$, the wave function must transform into the quasiclassical solution in the external region, which does not contain Z directly. Using this approximation for the order of magnitude for $r\sim a/Z$ as well, we find that

$$\psi\left(\frac{a}{Z}\right)\sim\sqrt{Z}.$$

Since for $r\ll a/Z^{1/3}$, the electron moves in the field of the unscreened nucleus with charge Z, its wave function in this region differs from a hydrogen-like wave function only in normalization, and in addition, its argument is rZ/a. It is therefore clear that for $r\ll a/Z$, and in particular, for $r\to 0$, assuming that the function ψ does not vanish there, the following estimate is also valid:

$$\psi(0)\sim\sqrt{Z}. \tag{14}$$

This increase with Z in the values of the wave function of the valence of electron near the nucleus is well-known and has been observed experimentally, for example, from the Z-dependence of isotopic mixing in heavy atoms and of the hyperfine structure. At short distances, near the unscreened nucleus, the speed of the electron also increases linearly with Z:

$$\frac{p}{m}\sim Z\alpha. \tag{15}$$

The energy spacing separating the mixed levels is $\Delta E\sim m\alpha^2$. The factor R arises due to relativistic effects at small distances, which increase the attraction of the electron to the nucleus. This relativistic enhancement factor increases sharply for large Z and attains values ~10 for $Z\approx 80$. As a result,

$$\eta\sim\frac{Gm^2\alpha^2Z^3R}{\pi}. \tag{16}$$

The characteristic magnitude of the $E1$-amplitude is

$$A(E1)\sim ea=\frac{e}{m\alpha}. \tag{17}$$

The order of magnitude of the usual $M1$-transition is that of the Bohr magneton:

$$A(M1)\sim\frac{e}{m}. \tag{18}$$

Thus, for these transitions, the degree of circular polarization is

$$P\sim\frac{Gm^2\alpha Z^3R}{\pi}, \tag{19}$$

which constitutes a quantity of the order $\sim 10^{-7}$ for $Z\approx 80$.

Bouchiat's initial suggestion[13] referred to the strongly forbidden $M1$-transition $6s_{1/2}-7s_{1/2}$ in cesium. For an amplitude $A\,(M1)\sim 10^{-4}\,e/m$, we can expect a circular polarization $P\sim 10^{-4}$. It was then noted[17,18] that for similar transitions in thallium, due to the large value of Z, the circular polarization must be approximately an order of magnitude greater. Experiments appropriate for cesium and thallium are being carried out in France and the USA.

Another direction for the investigations was suggested in Refs. 19–21. We are talking about studying the optical activity of heavy metal vapors in the vicinity of the usual $M1$-transitions. It was in such an experiment involving bismuth[1] that the parity-nonconserving weak interaction of an electron and a nucleus was discovered.

The appearance of optical activity due to the weak interaction[2)] becomes obvious if we recall the spin ringlet discussed above. It is completely obvious that a gas of atoms that has such a structure rotates the plane of polarization of light in a manner similar to a sugar solution, the molecules in which are themselves shaped like spirals. But there is an essential difference between them: sugar molecules have two modifications, left and right, while atoms have only one modification.

[1)] The ideas presented below are, for the most part, taken from the book by Landau and Lifshitz.[16]

[2)] The fact that parity nonconservation leads to the appearance of optical activity was first noted by Ya. B. Zel'dovich.[12]

We note that the natural optical activity that we are discussing is a coherent[22] macroscopic manifestation of parity nonconservation. Indeed, the effect arises due to the difference in the refractive indices n_+ and n_- for right- and left-handed quanta, while the presence of a refractive index, more precisely, its deviation from unity, stems from the coherent forward scattering of light in atomic media. (The relation between the index of refraction and the forward scattering amplitude is derived, for example, in Ref. 16, § 142.) This difference in the refractive indices leads to a phase difference in the right- and left-handed components of a linearly polarized wave, and in addition, the angle of rotation of the plane of polarization is proportional to this phase shift, increasing linearly with increasing path length. The fact that the effect increases linearly with increasing dimensions of the system is what determines its macroscopic nature.

Let us express the magnitude of the optical activity of a substance in terms of the degree of circular polarization of radiation. An elementary analysis shows that the angle of rotation of the plane of polarization of light with wavelength λ along a path l is given by

$$\psi=\frac{\pi l}{\lambda}\operatorname{Re}(n_+-n_-). \tag{20}$$

We use the conventional definition adopted in optics, according to which the rotation is considered to be positive if the plane of polarization rotates in a clockwise direction from the point of view of an observer viewing the source. Since the degree of circular polarization P is nothing more than the relative difference in the interaction of left- and right-handed quanta with matter, it can be represented in the form

$$P\approx\frac{1}{2}\frac{\operatorname{Re}(n_+-n_-)}{\operatorname{Re}(n-1)}. \tag{21}$$

Substituting (21) into (20), we obtain the relation sought:

$$\psi=2\pi\frac{l}{\lambda}P\operatorname{Re}(n-1). \tag{22}$$

At first glance, formula (22) suggests that the effect could be made arbitrarily large by increasing l. However, in reality, this cannot happen due to light absorption. In order to estimate the optimum conditions for measurements, it is useful to represent the angle of rotation ψ as follows:

$$\psi=\frac{1}{2}\frac{l}{L}P\frac{\operatorname{Re}(n-1)}{\operatorname{Im}n}, \tag{23}$$

where the absorption length L is defined by the formula

$$L^{-1}=\frac{4\pi}{\lambda}\operatorname{Im}n. \tag{24}$$

The index of refraction and, as a result of relation (22), the optical activity as well attain maxima in the vicinity of an absorption line. In this region, the quantities $\operatorname{Re}(n-1)$ and $\operatorname{Im}n$ are comparable and

$$\psi\sim P\frac{l}{L}. \tag{25}$$

As already noted, the angle ψ is determined by the phase difference for right- and left-handed components of a plane polarized wave. For this reason, the fluctuation $\Delta\psi$ is related to the fluctuation in the number of photons detected $\Delta N\sim\sqrt{N}$ by the familiar uncertainty relation

$$\Delta\psi\sim\frac{1}{\sqrt{N}}.$$

Since the number of photons passing through the specimen being studied depends on its length l according to the law $N=N_0e^{-l/L}$, the statistical uncertainty in the magnitude of the degree of circular polarization, according to the relations presented above, amounts to

$$\Delta P\sim\Delta\psi\frac{L}{l}\sim\frac{1}{\sqrt{N_0}}\frac{L}{l}e^{l/2L}. \tag{26}$$

From here, it is easy to see that the minimum random error in measuring the effect is attained at $l\sim L$ (more precisely, $l=2L$). Under these conditions, for $\operatorname{Re}(n-1)\sim\operatorname{Im}n$

$$\psi\sim P.$$

For normal $M1$-transitions, lying in the optical region, it is easy to obtain a ratio l/L close to unity under real conditions. Thus, in these transitions, $\psi\sim P\sim10^{-7}$. For strongly forbidden $M1$-transitions, what we gain in the degree of circular polarization P in direct proportion to the dgree of forbiddenness, we lose quadratically in the absorption coefficient L^{-1} with other conditions remaining the same. For this reason, here, we lose a great deal as to the magnitude of the angle of rotation ψ.

We note that in an allowed $E1$-transition, the degree of circular polarization is negligibly small, since in expression (11) the amplitudes $A(E1)$ and $A(M1)$ exchange places, so that P turns out to be a factor of $\alpha^{-1}=137$ smaller, and not greater, than the mixing coefficient η. And, inasmuch as it is not possible to gain a noticeable advantage in the factor l/L, here, the angle of rotation ψ is also negligibly small. The optical activity is also extremely small in the vicinity of electrical quadrupole ($E2$)-transitions, inasmuch as in this case also the ratio of the added magnetic quadrupole ($M2$) amplitude to the principal amplitude $A(M2)/A(E2)\sim\alpha$, and not α^{-1}. Thus, normal $M1$-transitions are optimum transitions in the search for optical activity related to parity nonconservation.

d) Choice of objects in searching for optical activity

Let us begin with the requirements imposed on the light source. It is easy to show with the help of formula (26) that the light source must have sufficiently high intensity. Then, since the effect has a resonance character, this intensity must be concentrated in a band comparable in width with the absorption line. Finally, the light source must be tunable, in order to pick out the given line. (A more detailed discussion of these conditions is given in the next section.) Due to these requirements, tunable lasers are the most suitable light sources.[3)]

[3)] In this connection, we emphasize the fact that the study of the weak interaction of elementary particles in the optical experiments being discussed here was actually made possible by the vigorous development of laser technology in recent years.

The choice of suitable elements in searching for optical activity is determined by the presence in these elements of the usual $M1$-transitions from the ground state, lying in the visible part of the spectrum or near it, where tunable lasers operate, under conditions of large values of Z, and finally, appreciable vapor pressure at reasonable temperatures. These conditions are satisfied by thallium, lead, and bismuth ($Z = 81, 82, 83$, respectively). In a real situation, the ratio $\mathrm{Re}(n-1)/\mathrm{Im}\, n$ is of the order of unity in bismuth and can attain 60–70 in thallium and lead. Since the circular polarization attains $P \sim 10^{-7}$ in these elements, the angles of rotation attain magnitudes of $\sim 10^{-7}$ rad in bismuth and $\sim 10^{-5}$ rad in thallium and lead. However, from the point of view of suitable light sources, thallium and lead, in which the wavelength corresponding to the transitions discussed is $\lambda = 1.3$ μm, are less suitable for the time being.

e) Faraday effect

In concluding this section, we consider the serious problem presented by magnetic fields, which, as is well-known, also rotate the plane of polarization of light. If the rotation, caused by the parity nonconservation, arises due to the dependence of the refractive index n on the helicity of the photon, i.e., on its spin projection along the momentum, then magnetic rotation—the Faraday effect—arises due to the dependence of n on the projection of the photon spin on the direction of the magnetic field H. Since H is an axial vector, such a correlation, in contrast to the helicity, is a true scalar.

There are several mechanisms for the Faraday effect. We shall point out two such mechanisms that give the main contribution under real conditions. First, due to the Zeeman splitting of levels in a magnetic field, a difference arises in the resonant frequencies for right- and left-polarized quanta. The longitudinal magnetic field H, which in this manner imitates the effect of parity nonconservation, is estimated from the obvious relation $(e/m)H/\Delta < P$, where $\Delta = \omega - \omega_0$ is the displacement of the frequency of the light ω from the resonant frequency ω_0, while P is the degree of circular polarization from this, for $P \sim 10^{-7}$. The requirement $H < 10^{-4}$–10^{-3} G. The other, not so well-known, mechanism occurs in the presence of a nucleus with nonzero spin. In this case, the magnetic field mixes atomic hyperfine states with different total angular momenta F, but with the same value of F_z. The limit on the field, following from the relation $(e/m)H/\Delta_{HF} < P$, where Δ_{HF} is the hyperfine splitting, is as follows: $H < 10^{-3}$ G. We note that similar to the rotation arising from parity nonconservation, and in contrast to Zeeman rotation, this effect is an odd function of the detuning Δ.

4. EXPERIMENTAL INVESTIGATION OF THE WEAK INTERACTION OF ELECTRONS AND NUCLEONS

a) Brief overview of experiments

Although the first realistic suggestions for searching for parity nonconservation effects in atoms involved measuring circular polarization in strongly forbidden $M1$-transitions, experiments involving cesium and thallium have not yet achieved the required precision. Up to now, these experiments, carried out in France and in the USA, yielded the amplitudes of the transitions themselves.[23,24] As far as the degree of circular polarization is concerned, the results of the experiments in thallium[25] do not contradict theoretical predictions,[29,30] but the random error in these experiments is of the same order of magnitude as these predictions. According to the situation in September 1979, the statistical error in the experiment with cesium[26] also equals the theoretical predictions.[27,28] However, the authors have not as yet presented the results of the measurements.

Experiments searching for the effects of parity nonconservation in atomic hydrogen and deuterium are at present being undertaken by several groups. These experiments are extremely difficult. We will not stop to consider them, but refer the reader to the original work.[31-35]

Experiments searching for natural optical activity were proposed almost simultaneously at the Institute of Nuclear Physics (Novosibirsk, USSR),[19] Oxford University (Oxford, England)[20] and at the University of Washington (Seattle, USA).[21] In Novosibirsk, preparations for the experiment began during the summer of 1974. Preparations were undertaken in Seattle and Oxford at approximately the same time. Bismuth was chosen for the experiments in all laboratories.

The ground state of the bismuth atom belongs to the configuration $6p^3$, i.e., it has three external p-electrons outside filled shells. The normal $M1$-transitions are possible only between levels belonging to the same electronic configuration. The diagram of such transitions out of the ground state of bismuth is shown in Fig. 2.

The results of calculations of the degree of circular polarization of radiation emitted in these transitions are displayed in Table I. For completeness, the values of this quantity for the normal $M1$-transitions in thallium and lead are also given in the Table.

In Novosibirsk and Oxford, the red line of bismuth ($\lambda = 648$ nm) was chosen for the experiment due to the fact that a reliable tunable continuous dye laser with a quite narrow line is available as a light source at this frequency. The disadvantage of this transition is that it lies in a region overlapped by the quite dense spectrum of molecular bismuth (the partial pressures of the atomic and molecular bismuth vapors are approximately equal). This disadvantage is absent for the infrared line ($\lambda = 876$ nm), near which the molecular spectrum is very

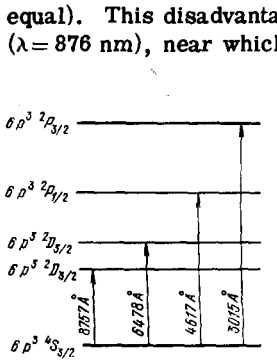

FIG. 2. Diagram of $M1$-transitions in atomic bismuth.

TABLE I. Circular polarization of radiation for thallium, lead and bismuth (all numbers are presented for $\sin^2\theta = 0.25$).

λ, nm	Tl	Pb	Bi				Reference
	1283	1279	876	648	462	301	
$P \cdot 10^7$	3.4	2.4	2.9	3.8	6.5	8.3	38, 37
	2.8		3.6				36
			2.4	2.8			39
	4.3						30
			2.4				40

weak. For this reason, this line was chosen for the work in Seattle,[41] in spite of the fact that it was necessary to use a pulsed laser with a fairly broad line (parametric oscillator).

Experiments searching for optical activity are also being carried out at the Lebedev Physical Institute in Moscow.[42]

b) Scheme for measuring small angles

How can negligibly small angles of rotation of the plane of polarization, of the order of 10^{-7} rad, be measured? It would seem that it is enough to place the specimen under study between crossed polarizer and analyzer and then determine this angle from the intensity of the transmitted light as follows

$$I' = I \sin^2\psi \approx I\psi^2,$$

where I is the intensity of light incident on the analyzer. However, under real conditions, the situation is not so simple. The problem is that with crossed polarizer and analyzer the intensity of the transmitted light does not exactly equal zero, but is diminished by only a factor of 10^7 at best. Evidently, under such conditions, it is practically impossible to record the negligibly small change in the intensity of light caused by the rotation of the plane of polarization by an angle $\sim 10^{-7}$ rad. Moreover, since the observation of such angles involves a long signal accumulation time, all the possible displacements in the optical elements and electronics also make such measurements practically impossible.

Schemes that actually measure small angles make use of the modulation technique. In this method, a reference angle θ is added to the angle ψ, so that the intensity of the transmitted light equals

$$I' = I\,[\sin^2(\theta + \psi) + \delta^2] \approx I\,(\theta^2 + 2\theta\psi + \delta^2), \qquad (27)$$

where $I\delta^2$ is the intensity of the light transmitted through crossed polarizer and analyzer.

In the standard procedure, the reference angle is modulated with the help of a Faraday cell. The light from the source passes through the polarizer, Faraday cell, specimen being studied, and analyzer; the latter transmits light with polarization orthogonal to the polarizer, which is then detected by a photodetector. The Faraday cell consists of a transparent (to the light) substance with a quite high Verdet constant (heavy flint glass distilled water, and so on), placed in an alternating longitudinal magnetic field. The frequency of the alternating magnetic field used usually lies in the range from 0.1 to 1 kHz. Thus, the signal from the photodetector is proportional to

$$V \sim I\,(\theta^2 \sin^2\Omega t + 2\theta\psi \sin\Omega t + \delta^2), \qquad (28)$$

where Ω is the frequency of modulation of the reference angle. The fundamental of this frequency in the signal from the photodetector, proportional to the measured signal, is recorded with a synchronous detector.

In order to study optical activity resulting from parity nonconservation, a new frequency-modulation measurement technique was developed to Novosibirsk.[43,44] In this scheme, the wavelength of the light is modulated, so that if parity is not conserved, then, as the wave passes through resonance, the angle of rotation of the plane of polarization ψ_{PNC} changes sharply (Fig. 3). In the scan of the wave symmetrically relative to the absorption line center, the intensity of light transmitted through the analyzer

$$I' \approx I(t)\,\theta^2\left(1 + \frac{2\psi_{PNC}}{\theta} + \frac{\delta^2}{\theta^2}\right), \qquad (29)$$

contains the fundamental (more precisely, odd harmonics) only in the presence of parity nonconservation, since $I(t)$ has only even harmonics. For small scanning amplitudes, the signal of the fundamental is proportional to $\partial\psi_{PNC}/\partial\lambda$. Thus, in contrast to the usual schemes for measuring small angles of rotation of the plane of polarization, the scheme proposed here actually measures the derivative of these angles with respect to wavelength.

In the preceding discussion, it was tacitly assumed that the angle θ between the polarizer and analyzer axes is small. In order to choose an optimum value for this angle, let us consider how the effective signal-to-noise ratio depends on this angle. Assuming that the noise is purely random in nature, while the optical system is an ideal system, this ratio does not depend on the angle θ, since both the effective signal $I\theta\psi$ and the random noise $\sqrt{I\theta^2}$ are proportional to θ. However, as mentioned above, due to the nonideal nature of the polarizer and analyzer, the intensity of the light transmitted through them for $\theta = 0$ is $I\delta^2$. For this reason, the use of angles θ less than δ degrades the effective signal-to-noise ratio. On the other hand, for angles θ greater than δ, the relative magnitude of the effective signal in the measuring channel decreases and this imposes stricter requirements on the electronics and on the tolerable magnitude of various spurious effects. Starting with these considerations, angles θ lying in the range from 10^{-3} to $4 \cdot 10^{-3}$ rad were used in the experi-

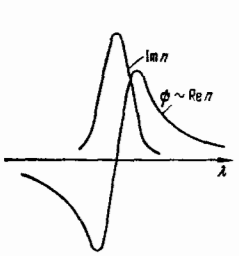

FIG. 3. Expected wavelength dependence of the angle of rotation of the plane of polarization and of the absorption of light in the vicinity of a $M1$-transition.

ment. The scheme of the experiment for measuring the optical activity of bismuth vapor is shown in Fig. 4. The light source consisted of a model 375 Spectra Physics tunable dye laser. This laser has a line width of about 0.1 Å and does not allow for rapid wavelength scanning. In order to use the technique proposed above, it was necessary to tune the laser wavelength rapidly and to have a much narrower line. For this purpose, a new method was proposed and realized for selecting longitudinal laser modes.[45] An additional element was introduced into the laser: a selector that provided a single-frequency tuning regime with output beam power of 15 mW. The use of the selector permitted discrete wavelength scanning with a step size of 0.006 Å scanning frequency up to several kHz, and scanning amplitude up to 10 Doppler line widths. Actually, in the experiment, the scanning frequency was chosen as 1 kHz, while the amplitude was chosen as 1 to 2 Doppler widths. The light, modulated according to wavelengths with a frequency 1 kHz, passed through the polarizer, the cell with the bismuth vapor, and the analyzer. The polarizer and analyzer consisted of prisms made of icelandic spar with an apex angle of 12°. The axes of the polarizer and analyzer were positioned at an angle of θ to one another. A special mechanical system permitted changing the sign of the angle θ.

The analyzer splits the beam into two beams with mutually orthogonal polarizations, one of which is a factor of θ^{-2} weaker than the other. Each of the two beams was detected by a FÉU-79 photomultiplier (quantum yield of 5% at $\lambda = 648$ nm). Special cavities were placed in front of the photomultipliers for diffuse scattering of light. Without them, the nonuniformity of the photocathodes, together with variations in the structure and displacement of the laser beam accompanying the wavelength tuning, cause large spurious effects. A gray filter with an attenuation coefficient $\approx 10^3$ was placed in front of the FÉU-1 photocathode, which recorded the bright beam, in order to partially smooth out the intensities.

The signals from the photomultipliers depend on θ and ψ_{PNC} as follows:

$$V_1(t) \sim I(t)\cos^2(\theta + \psi_{PNC}(t)) \approx I(t), \tag{30a}$$

$$V_2(t) \sim I(t)\sin^2(\theta + \psi_{PNC}(t)) \approx I(t)\,\theta^2\left(1 + \frac{2\psi_{PNC}(t)}{\theta}\right). \tag{30b}$$

Since the signal from the FÉU-1 does not depend on the effect being measured when scanning the laser symmetrically relative to the center of the line, the signal must only contain even harmonics of the scanning frequency. Since the optical length of the bismuth vapor in the experiment equals several absorption lengths, V_1 depends very strongly on time. For this reason, with imprecise tuning on the center of the absorption line, the fundamental of the scanning frequency appears in the signal V_1. Depending on which side of line center the shift occurred, the phase of the fundamental of the signal changes by 180°. The signal V_1 was synchronously detected at the fundamental of the scanning frequency, amplified, and fed into the laser selector for automatic tuning of the wavelength. This feedback ensured the absence of the fundamental in $I(t)$ to a level not exceeding 10^{-3}.

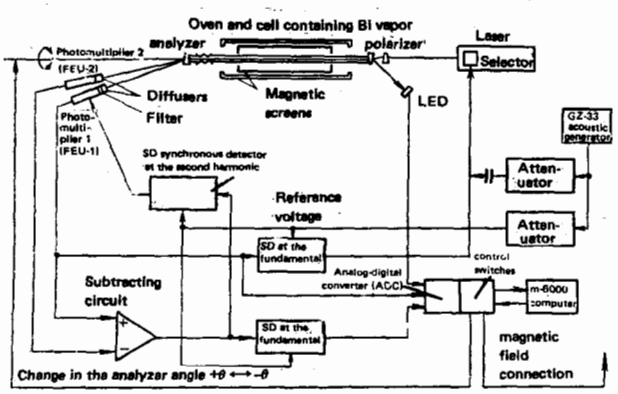

FIG. 4. Block diagram of the experiment.

The voltage on the photomultipliers was chosen so that the signals V_1 and V_2 would be practically equal to one another. These signals were fed into a subtracting circuit. In the case that the signals are equal, the difference signal $V \sim I(t)\theta\,\partial\psi_{PNC}/\partial\lambda$ can contain the fundamental only through the wavelength dependence of ψ_{PNC}. In order to maintain high precision in subtracting V_1 and V_2, we used the fact that if they are unequal, the amplitude of the second harmonic, the phase of which depends on which the signals V_1 or V_2 is greater, appears in the signal V with a large amplitude. The difference signal V was synchronously detected at the second harmonic of the scanning frequency; it controlled the voltage supply to the FÉU-1 photomultiplier. This feedback provided better than 10^{-3} precision in subtracting.

As a result of the use of both types of feedback, the spurious signal at the fundamental must correspond to an effective rotation angle $2\psi_{eff}/\theta \leq 10^{-6}$ [see formula (30)], which for angles θ used constituted $\psi_{eff} \leq 10^{-9}$ rad.

However, in the experiment, the level of the fundamental in the signal was determined with other methods besides electronic methods, as will be seen from what follows. For additional suppression of spurious signals, the measurements were performed alternately for two values, $+\theta$ and $-\theta$, of the reference angle. The difference of the average values V_+ and V_- for these two cases serve as a measure of parity nonconservation. The angle of rotation was determined from the relation $\psi_{exp} = (\partial\psi/\partial\lambda)\Delta\lambda$ and related to the results of the measurements as follows:

$$\frac{4\psi_{exp}}{\theta} = \frac{V_+ - V_-}{V_s K},$$

where K is the amplification factor of the subtraction circuit and the synchronous detector at the fundamental.

c) Description of setup

An oven, the construction of which is shown in Fig. 5, was used to obtain bismuth vapor. The oven operated on the heat pipe principle. A cell with bismuth vapor was connected to a large ballast volume, filled with helium. As the oven was heated, when the temperature in the cell attained a value at which the pressure of the saturated bismuth vapor equalled the helium pressure in the system, helium was pushed out and only bismuth

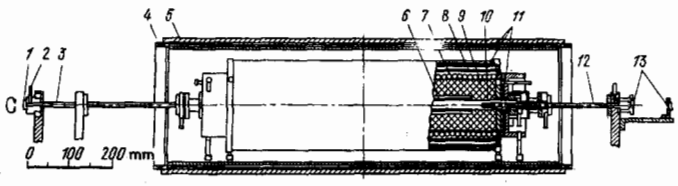

FIG. 5. Oven and cell with bismuth vapor 1—analyzer prism; 2—helium inlet; 3—moving seal; 4—coil; 5—steel housing; 6—heater; 7—cooler; 8—sectioned coil; 9—thermal insulation; 10—ceramic cell; 11—magnetic screens; 12—collimator; 13—polarizer prism.

vapor remained in the center of the cell. In such a system, when the power input is changed, the temperature and the corresponding vapor pressure do not change, only the length of the region occupied by vapor changes. The polarizer and analyzer prisms served as the input and output windows of the cell. Cold helium at the ends of the cell protected them from bismuth deposits.

To avoid creating a constant magnetic field, which rotates the plane of polarization and can imitate the parity nonconservation effect, a 50 Hz alternating current was fed to the heater. In order that the alternating field in the system be small as well, the heater was shaped in the form of a double spiral. To suppress external magnetic fields, the oven and cell were placed in a double magnetic screen consisting of annealed Permalloy, which reduced the magnetic field at the center of the cell to less than $2 \cdot 10^{-5}$ G. The use of correcting coils, positioned at the ends of the external screen, ensured a field with this value along a length of up to 60 cm. The magnetic field was measured by ferromagnetic probe sensors.[46]

In the construction of the setup, measures were taken to avoid contacts with different metals, which eliminated magnetic fields due to thermoelectromotive forces not otherwise would have arisen with heating of the oven. The final criterion ensuring a small residual field in the heated cell was the absence of magnetic rotation for measurements with those atomic lines for which Faraday rotation exists, while the effect stemming from parity nonconservation is known to be absent.

An additional coil, consisting of seven sections, which was used to measure the bismuth vapor density distribution along the cell axis, was placed inside the screen. For this purpose, in the case of alternate switching in of the coil sections, the Faraday rotation was measured for lines in which this rotation is large.

The electronic part of the apparatus contains a series of specially developed devices.[45] The blocks indicated in Fig. 4 as synchronous detectors include narrow band amplifiers at frequencies 1043 and 2086 Hz, respectively. The integration time of the synchronous detectors and the total amplification factor of the effective signal at the fundamental from the FÉU-2, allowed for in the circuit, were often adjusted in discrete steps at the early, most difficult, stages of the experiment.

In later measurements, an automatic system was used for control, monitoring, data collection, and data processing, realized in the KAMAK format and fed into a M-6000 computer. A signal from the synchronous detector at the fundamental, proportional to the effect being measured, and the intensities of the incident and transmitted light were fed through an analog-digital converter (ADC) into the computer memory. A special rapid ADC block[47] recorded the information concerning the shape of the absorption line. The block containing the control switches was programmed to change the angle of the analyzer prism $+\theta \rightleftharpoons -\theta$ and also controlled the circuits that changed the phase at which the heating element of the oven was fed by 180° synchronously with the change in the angle θ. The phase of the heater was changed for the following reasons. The heating element created a small alternating magnetic field with a frequency 50 Hz along the axis of the cell containing the bismuth vapor. The 1 kHz carrier frequency also is slightly modulated at a frequency of 50 Hz. As a result, this alternating Faraday rotation in bismuth vapor can be recorded as an effect. Special measures were adopted for revealing and suppressing this pickup. Since the difference of the first harmonic for the $+\theta$ and $-\theta$ positions of the reference angle serves as the effective signal, the synchronous change in phase in feeding the heater and angle automatically subtracts out the spurious signal indicated. The program allowed for operation in a regime in which both the parity nonconservation effect and the Faraday rotation were measured. The programs were triggered and the required parameters were input from a videotron.

d) Measurements and analysis of results

Although the work was begun during the summer of 1974, the dye laser was not delivered until April 1976. By then, the electronic equipment, oven, and system of magnetic screens were prepared. By the end of 1976, the laser was significantly modified and it was put into a single-frequency tunable lasing regime. After this, the absorption spectrum of bismuth vapor was measured in the region of several angstroms, where the lines of the hyperfine structure for the transition at 648 nm should be observed.

The transition $^4S_{3/2} - {}^2D_{5/2}$, for which the parity nonconservation measurements were made, can proceed as a magnetic dipole and as an electric quadrupole transition. Since the spin of the bismuth nucleus equals $\frac{9}{2}$, the hyperfine structure of this transition consists of 12 lines with $\Delta F = 0, \pm 1$ and 6 lines with $\Delta F = \pm 2$. The lines with $\Delta F = 0, \pm 1$ correspond to magnetic dipole transitions with a mixture of quadrupole transitions. The parity nonconservation effect was measured for these transitions. Transitions with $\Delta F = \pm 2$ are purely quadrupole transitions, so that the effects of parity nonconservation are approximately a factor of $\alpha^2 \sim 10^{-4}$ less here. These effects are also strongly suppressed in the molecular lines of bismuth, for which the partial vapor pressure at temperatures $\approx$1200 °C is approximately equal to the pressure of atomic bismuth.

Figure 6 shows the absorption curve for bismuth vapor measured in the vicinity of the $^4S_{3/2} - {}^2D_{5/2}$ transition. As evident from the figure, the hyperfine structure is masked by the strong absorption spectrum of molecular bismuth, so that it is impossible to find the

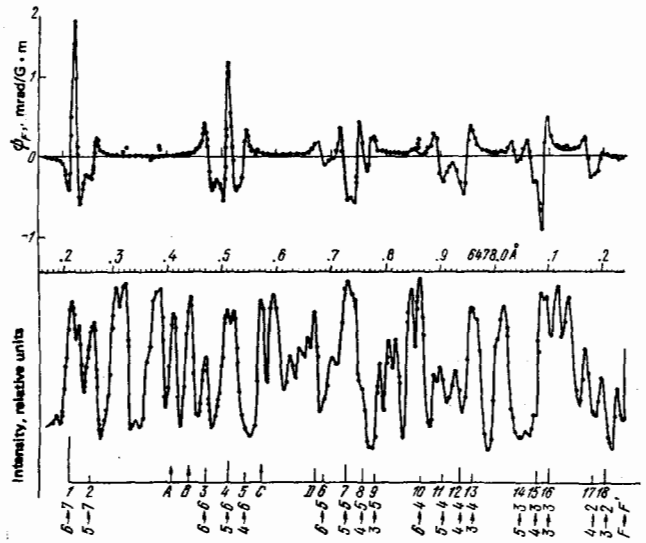

FIG. 6. Faraday rotation and absorption spectrum of bismuth vapor in the vicinity of the $\lambda = 649$ nm transition.

position of the atomic lines from the known spacing between the hyperfine components, first measured in 1942 and 1946 by Mrozovski.[48] They were identified by measuring the Faraday effect in this region of the spectrum.

The standard scheme was used to measure the wavelength dependence of the Faraday rotation. The advantage of this scheme lies in the fact that in contrast to the frequency modulation technique, it permits making measurements at points other than the maxima and minima in the intensity of the transmitted light. Since we are concerned here about measuring angles $\sim 10^{-4}$ rad, in this case a serious disadvantage of the standard scheme is not important, namely, the presence of an additional substance between the polarizer and the analyzer, at least a Faraday cell, which can cause various spurious effects. The setup was restructured in accordance with the change in the experimental scheme. A Faraday cell, which modulated the reference angle at a frequency of 1 kHz, was placed between the polarizer and the cell containing the vapor. In addition, the laser wavelength was scanned at a frequency of 0.01 Hz.

Figure 6 shows the results of measurements of the Faraday rotation for the atomic transition $^4S_{3/2} - {}^2D_{5/2}$. The figure also shows the curve of the effect computed by O. P. Suchkov and V. V. Flambaum based on Refs. 49 and 37. For the calculations, the reduced amplitude of the $M1$-transition was taken as equal to $0.55\ e/2m$, as obtained in Ref. 37; the error in this number does not exceed 2%. The partial pressure of the atomic bismuth vapor was determined by comparing the measured and computed Faraday angles; the value obtained agrees within the 5–10% precision of the measurements with the handbook value.[111]

Comparison of the theoretical and experimental results gives the following values for the free parameters of the calculation: the impact broadening of the lines does not exceed several percent of the Doppler width; the radial integral for the amplitude of the $E2$-transition $\langle r^2 \rangle = (9.0 \pm 0.6) a^2$, and the constants for the magnetic dipole and quadrupole hyperfine splitting of the $^2D_{5/2}$ level are $A = 2503.8 \pm 1.6$ MHz and $B = 2 \pm 23$ MHz. The indicated value of $\langle r^2 \rangle$ agrees with results obtained at Oxford[50] from measurements of the Faraday effect under conditions of large impact broadening. Somewhat better precision in determining the constant B was obtained in the recent work described in Ref. 51: $B = 14 \pm 11$ MHz. The computed value of this constant[52] is $B = 8.5 \pm 7$ MHz.

We shall consider the data obtained from the analysis of the Faraday effect in detail because of the fact that they are used for quantitative interpretation of the results of the parity nonconservation measurements. These data on the Faraday effect were obtained with the use of the automated data collecting and processing system.

The first curves of the Faraday rotation were obtained with a less perfected setup. However, even these curves permitted establishing reliably and uniquely the position of the hyperfine structure lines of atomic bismuth relative to the absorption spectra and to go on immediately to a study of parity nonconservation. The measurements were begun on the control molecular lines. In the setup of that time, the input and output windows of the cell consisted of glass, Franck-Ritter prisms were used for the analyzer and polarizer, in which one of the polarization components of the light was extinguished, and beam splitting plates and mirrors were used to obtain an intense light beam incident on the FÉU-1. A Faraday cell was used to change the angle $+\theta \rightleftharpoons -\theta$. There were no light diffusers in front of the photomultipliers. The first measurements with the control molecular lines gave signals, imitating parity nonconservation, at levels approximately a factor of 10^3–10^4 greater than expected for the working lines. Microscopic displacements of any element in the setup changed the sign of the signals. After a while it was clear what caused the observed phenomena. When the wavelength is scanned, the spatial structure of the laser beam is restructured synchronously. When the modulated light reaches the photomultipliers, the nonuniformity of the photocathodes generates the fundamental. In order to suppress this effect, cavities, which were painted inside with a diffusely scattering paint, were positioned in front of each photomultiplier. The cavities had two openings, one for letting in the laser beam and the other for letting out the diffusely scattered light toward the photocathode. The cavities mixed the light well, so that even with significant displacements of the photomultiplier with the diffuser relative to the laser beam, no changes were observed in the signal at the fundamental. The use of the diffusers reduced the signal at the fundamental by 3 to 4 orders of magnitude, but effects comparable with those expected for the working lines were still observed with the control lines. The remaining spurious effects still stemmed from the synchronous restructuring of the beam. The problem is that all optical elements create ellipticity, which is nonuniform across the surface, and as a result with synchronous tuning of the beam, a fundamental signal, which, moreover, changes in time as the beam drifts smoothly or the beam struc-

ture is altered. Plane parallel glass, positioned along the beam axis, also created big problems. Thus, for example, an attempt was made to use interference light filters in order to suppress light from the oven. In doing so, a smooth variation with a period of about one hour was observed in the signal at the fundamental. It turned out that it was caused by a slow displacement of the light filter, fixed in place with the help of modeling clay. Reflected light entering the laser was especially dangerous; even when the reflected light was attentuated by a factor of 10^5, uncontrollable feedback coupling could not be avoided in the system. Further work primarily consisted of simplifying the optical scheme. As a result, nothing was left between the polarizer and analyzer besides the bismuth vapor and helium.

Preparations of the apparatus for a run of measurements began with work on the molecular line with the greatest width. This permitted increasing the scanning amplitude by a factor of 4–5 in comparison with the normal operation. This increased the effects related to synchronous restructuring of the laser beam. The intensity of the laser light also increased in comparison with the working intensity approximately by an order of magnitude (at the same time, laser generation occurred at several longitudinal modes). All this permitted a decrease in the time required for the observations. Under such conditions, by displacing the polarization prisms, we achieved minimal spurious effects. After this, the prisms, lenses, diaphragms, and so on were not displaced in any way during the run. During the run, measurements at the working and control lines were alternated. At the end of each measurement, a magnetic field of $\sim 10^{-2}$ G was switched on. The value of the angle of rotation of the plane of polarization with the magnetic field switched on, measured by the same frequency modulation method, served as a check on the operation of the apparatus and was used to normalize the parity nonconservation effect. Such alternating measurements on a group of working and control lines constituted a single run. In preparing for the first three runs, the amplitude of the fundamental in the difference signal was not always stable in time. As a result, preparation for a run sometimes took about one month.

In all, three series of measurements were carried out. The first series consisted of a single run, and the second and third consisted of two runs each. Between the series of measurements, the setup was repeatedly modified. In doing so, at least two goals were pursued: the first goal was to achieve stable operation or at least to increase the time over which the system behaved smoothly; the second was to eliminate possible systematic errors. For example, in the first series of measurements, the polarizer was rotated by an angle $\pm\theta$; the polarizer was made in such a way that when it was rotated the position of the light beam on the photomultipliers did not change. In the second series, the analyzer was rotated, and the photomultipliers were stationary. In the third series of measurements, the photomultipliers were rotated instead of the analyzers so that the relative position of the light beams and the photomultipliers did not change. The axis of rotation of the photomultipliers and the analyzer prisms coincided with the axis of the laser beam inside the cell so that rotation of the analyzer prism did not cause a displacement of the light beam across the prism. As already mentioned, the third series of measurements was automated. During the operation of the system, the system of diaphragms, their dimensions, and their mutual positioning were changed significantly. Successive improvements in the system resulted in the fact that in the last measurments no instability was observed in the signal at the fundamental.

In the first series, measurements were carried out on seven lines.[1] Rotation of the plane of polarization of light could be expected for four of these (lines 1, 3, 7, and 12 in Fig. 6). Three lines (two molecular and one quadrupole, A, C, and 10 in Fig. 6, respectively) serve to check the operation of the apparatus. In this series of measurements, the polarizer was rotated by an angle $\pm 1 \cdot 10^{-3}$ rad. The sign of the angle was changed every 200 s, and in doing so, in order to eliminate transient processes, the first 50 s following the switchover of the polarizer were not used in the analysis of the results. The integration time of the synchronous detectors in this session was equal to 15 s. Ten measurements were performed for each line for each position of the polarizer. The total amount of time for the measurements per line, including the measurements with the magnetic field switched on, constituted about 1.5 hours. The signals that are proportional to the measured effect, the intensities of the incident and transmitted light, as well as the feedback signals were recorded on a five-channel automatic plotter. In the first series of measurements, the average angle of rotation for lines corresponding to the $M1$-transitions $\Delta F = 0, \pm 1$ constituted $(-6.7 \pm 1.6) \cdot 10^{-8}$ rad, while the average angle of rotation for the control lines equalled $(2.1 \pm 1.5) \cdot 10^{-8}$ rad. This result demonstrates uniquely parity nonconservation in atoms, since the average angle of rotation for the working lines differs from zero by more than four standard deviations.

In carrying out this series of measurements, there was no sectioned coil inside the magnetic screen, which did not permit determining the length of the region occupied by the vapor from the Faraday rotation. This length was roughly estimated according to the position of the locations at which condensation of bismuth occurred. It was also impossible to normalize sufficiently well the measured effect from the magnetic measurements. The problem is that Faraday rotation is very sensitive to the position of the modes generated by the laser relative to the atomic bismuth lines, which was not known with sufficient precision in this series of measurements. Taking these circumstances into account, when comparing the result obtained with the predictions based on the Weinberg–Salam model, an additional factor K, which took into account the uncertainty in the normalization of the effect and in order of magnitude fell into the range 0.5 to 1.5, was introduced. The average value of the ratio of the measured angles to the angles computed on the basis of Ref. 36, according to the results of this series of measurements, constituted

$$\left\langle \frac{\psi_{exp}}{\psi_{theor}} \right\rangle = (1.4 \pm 0.3) K. \quad (31)$$

In the second series,[2] the measurements were performed with the working lines 1, 3, 7, 12, and 18, while measurements with lines 2, *A*, *B*, *D*, and 17 (see Fig. 6) served as a check. In this series of measurements, the analyzer was rotated by an angle $\pm 2.5 \cdot 10^{-3}$ rad, somewhat greater than the rotation of the polarizer in the first series. A sectioned coil, with the help of which the density distribution of atomic bismuth vapor along the cell axis was measured from the magnetic rotation, was placed inside the magnetic screen. The procedure for making the measurements in this series was the same as in the first series, but the shapes of the absorption lines in the bismuth vapor were determined more carefully.

Coefficients transforming the results from one series of measurements to the other were computed by comparing the measured magnetic rotation angles for the same lines in the first and second series. It should be noted that the wavelength scanning amplitude, which changes the magnitude of the effect expected, was greater in the second series than in the first. Data from the first series, referred to the conditions of the second series of measurements, were added to the results of the second series and were processed simultaneously. As a result, the average rotation angle at the working lines consituted $(-3.1 \pm 0.5) \cdot 10^{-8}$ rad, and $(1.0 \pm 0.5) \cdot 10^{-8}$ rad at the control lines. As can be seen from Fig. 7, due to the contribution of the wings of *M*1-transitions, a small effect should also be observed with the control lines, and with opposite sign, since the regions of anomalous and normal dispersion have opposite signs. The average expected angle of rotation for the control lines constitutes about $0.2 \cdot 10^{-8}$ rad. The line-averaged value of ψ_{exp}/ψ_{theor}, obtained from these measurements, turned out to equal

$$\left\langle \frac{\psi_{exp}}{\psi_{theor}} \right\rangle = 1.04 \pm 0.28. \quad (32)$$

This number differs by 6% from that presented in Ref. 2, which is connected with the fact that here, in calculating ψ_{theor}, the more precise value[37] (0.55 $e/2m$) was used for the reduced amplitude of the *M*1-transition.

The relative error in (32) is somewhat greater than in the value of the average angle of rotation for the working lines, since the expected result includes not only random errors, but also errors related to the remaining uncertainty in the position of the generated laser modes relative to the atomic lines of bismuth.

Before the third series of measurements,[53] the setup was greatly altered. This series of measurements made use of an automatic system for controlling the experiment and for collecting information. An electromechanical system was installed for switching the analyzer angle, the magnitude of which was increased to $4 \cdot 10^{-3}$ rad. The photomultipliers were turned together with the analyzer. In this series, the integration time was decreased to 1 s and the signals from the output of the synchronous detector and the integrated signals of the incident and transmitted light intensity were measured and recorded in computer memory every 0.1 s with the help of the ADC. The block containing the special rapid ADC recorded, synchronously with the frequency of wavelength scanning, the instantaneous values of the transmitted light intensity at 256 points with a step of 5 μs. These measurements were repeated 400 times at intervals of 0.1 s and after this, the sign of the angle θ was automatically changed. In order to eliminate the influence of transient processes, the first 100 measurements after the angle was switched were excluded from the data analysis. In all, for each measurement on a line, the analyzer angle was switched 20 times (20 pairs), after which measurements performed with a magnetic field of $\pm 10^{-2}$ G switched on. Twenty six such measurements, alternating between the working and control lines were made on the lines 1, 2, and *A*, and 13 measurements on line 3, in the third series of experiments.

The data obtained in this manner were analyzed together with the results of the measurements of the Faraday curve and the absorption spectrum, similar to data obtained in the region of the first two groups of hyperfine structure lines for the transition $^4S_{3/2} - {}^2D_{5/2}$ (see Figs. 7a and b). As a result, the positions of the generated laser modes relative to the atomic lines and the intensity of the transmitted light for fixed wavelengths

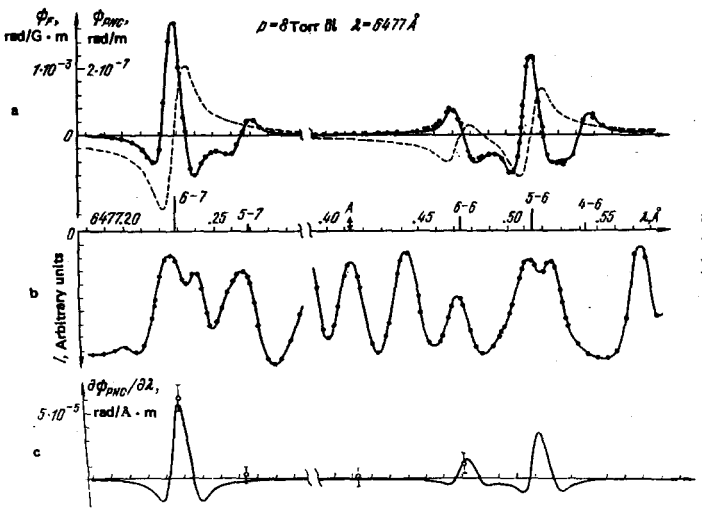

FIG. 7. a) Dashed curve—theoretical prediction of the optical activity of bismuth vapor; solid curve—calculated Faraday rotation. b) Calculated curve $\partial\psi_{PNC}/\partial\lambda$ and the results of the last series of measurements.

were determined with sufficient precision. The expected values of the angles were compared from theoretical curves of the expected effect and of the Faraday rotation for each laser mode generated. The results were further processed with these values and values of ψ_{exp}/ψ_{theor} were obtained.

The results of the measurements performed in this series are shown in Fig. 7c. As can be seen from the figure, the measurements on the control lines indicate the absence of systematic errors, in particular, those related to residual magnetic fields. Measurements on the working lines yielded the following result:

$$\left\langle \frac{\psi_{exp}}{\psi_{theor}} \right\rangle = 1.09 \pm 0.17. \quad (33)$$

This time, the error shown is purely random. As far as the first two series of measurements are concerned, we emphasize once again that although their errors exceed the random errors, this difference stems only from the normalization of the results of the measurements and not from spurious signals that could imitate parity nonconservation.

As evident from the data presented, the results obtained in the entire series of measurements agree well with each other. It should once again be emphasized that in all the series of measurements, the measurements were performed under different conditions, in particular, different polarizers and analyzers were used in different series. This permits considering the results obtained in the three series independently. Averaging the results obtained in the three series of measurements, we obtain

$$\left\langle \frac{\psi_{exp}}{\psi_{theor}} \right\rangle = 1.07 \pm 0.14, \quad (34)$$

or, using the notation most often encountered in the literature, $R = -P/2$,

$$R = (-20.2 \pm 2.7) \cdot 10^{-8}. \quad (35)$$

Thus, the results obtained at the Institute of Nuclear Physics in Novosibirsk prove that parity is not conserved in atomic transitions and these results quantitatively confirm the Weinberg–Salam model.

It is well-known that the results obtained in Novosibirsk contradicted the Oxford[54,55] and Seattle[54,56,57] data published up to that time. Since then, the situation has changed. At the present time, the Oxford group definitely sees an effect at the level predicted by the Weinberg–Salam model. Their new apparatus eliminates a series of possible systematic errors, which could have effected the previous results. The investigation of systematic errors continues. The most recent result of the Oxford group[58] is $R = -(10 \pm 2) \cdot 10^{-8}$. In Seattle, new measurements of optical activity of bismuth vapor were performed on the infrared line $\lambda = 876$ nm using semiconducting lasers. The results of those measurements have been reported[59]: $R = -(10 \pm 1) \cdot 10^{-8}$, which does not contradict the Weinberg–Salam model (see above, Table I). However, as pointed out by the authors, the measurements still contain some systematic errors. The most recent result of this group[113] is $R = -(9.5 \pm 1.2) \cdot 10^{-8}$.

Recently, the first reports of the measurement of optical activity of bismuth vapor in the red line, carried

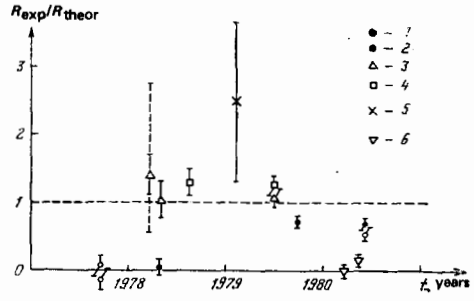

FIG. 8. Chronological sequence of the results of measurements of the parity nonconserving interaction of electrons with nucleons. R_{exp} is a parameter characterizing parity nonconservation; R_{theor} is the value expected from the Weinberg–Salam model with $\sin^2\sigma = 0.25$. 1—Seattle[56,57,59,112], 2—Oxford[55,58], 3—Novosibirsk[1,2,53], 4—Stanford[5,112], 5—Berkeley[25], 6—Moscow[114,115].

out at the P. N. Lebedev Physical Institute in Moscow, were published. The technique here is very similar to the one used in Oxford and Seattle. The first result of this group was[114] $R = (0.4 \pm 1.8) \cdot 10^{-8}$. Subsequent measurements gave[115] $R = -(4.0 \pm 1.8) \cdot 10^{-8}$ and $R = -(4.1 \pm 1.4) \cdot 10^{-8}$. Averaging these three results, the authors obtain[115] $R = -(2.3 \pm 1.3) \cdot 10^{-8}$, sharply contradicting the Novosibirsk data and the predictions based on the Weinberg–Salam model. Our confidence in the correctness of the Novosibirsk results is based on the fact that the technique that we used to perform the measurements has many advantages from the point of view of revealing systematic errors in the experiment. In particular, it permitted studying a large number of lines, both working and control lines.

Figure 8 shows in chronological order the results of measurements of parity nonconservation in the interaction of electrons and nucleons, obtained in different laboratories. The veritical scale shows the parameter that characterizes the ratio of the degree to which parity is not conserved and the predictions of the Weinberg–Salam model for $\sin^2\theta = 0.25$.

5. CALCULATION OF OPTICAL ACTIVITY OF THALLIUM, LEAD, AND BISMUTH VAPORS

Now that the optical activity of bismuth vapor has been measured with sufficiently high precision (~15%),[53] there arises the obvious question as to whether or not it is possible to extract quantitative information from these experiments concerning the interaction of elementary particles, or, in other words, how accurately is the degree of circular polarization in an atomic transition known, if weak interaction of electron and nucleus is assumed. Such considerations are all the more necessary since it is still widely believed that the reliability of all present calculations of the effects of parity nonconservation in atoms as complicated as bismuth is too low to obtain such information.

In order to demonstrate that such pessimism is groundless, we will consider the calculations carried out in Novosibirsk.[36,37] The idea of these calculations is to demonstrate the reliability of the results, without striving to achieve mathematical elegance, making use of the maximum possible number of experimental values

of atomic parameters. It is such a phenomenological approach, and not an *ab initio* calculation from first principles, that has allowed insisting that the precision of the Novosibirsk calculations is not worse than 20%, as far back as 1976, when the predictions of the other groups were greater than ours by a factor of 2.

As can be seen from expression (11), the calculation of circular polarization can be reduced to the calculation of the mixing coefficients η_n and amplitudes A_n ($E1$) and A ($M1$). The calculations were performed for thallium, lead, and bismuth. The ground states of these atoms belong to the configurations $6p$, $6p^2$, and $6p^3$, respectively. The states $6p^{k-1}$ ns with $n \geq 7$, including the continuous spectrum, and states of the type $6s6p^{k+1}$ involving excitation of the $6s^2$ subshell were taken into account as admixtures with opposite parity to the state $6p^k$.

For excitations of the type $6p^{k-1}$ ns, the situation in all three atoms is comparatively simple. In order to find the appropriate wave functions, we used the following spherically symmetrical effective potential[60]

$$U(r) = -\frac{\alpha}{r}\{1 + (Z-1)[H(e^{r/d}-1)+1]^{-1}\}, \tag{36}$$

in which the parameters H and d were chosen so that the position of the levels of the configurations $6p^k$ and $6p^{k-1}$ ns, including the fine structure, were correctly reproduced:

Tl	Pb	Bi
$Z = 81$	$Z = 82$	$Z = 83$
$H = 15.04$	$H = 14.04$	$H = 12.05$
$d = 1.58a$	$d = 1.54a$	$d = 1.40a$

(37)

The behavior of the wave functions near the nucleus, which is important for calculating the matrix element of the weak interaction, i.e., the mixing coefficient η_n, was checked by calculating the hyperfine structure constant (HFS). The results of this calculation for magnetic dipole HF splitting of the levels of the $6p^3$ configuration in bismuth[72] are displayed in Table II. The final theoretical values of the constants indicated in the table represent a single-parameter fit, and in addition, the free parameter x characterizes the admixture of the configuration $6s6p^3$ ns to $6s^26p^3$. This calculation also shows that the magnitude of this admixture does not exceed 3–4%. We note the fact that, as can be seen from Table II, the computed values of HF constants for the levels of the $6p^k$ configuration are very sensitive not only to the behavior of the wave function of the $6p$-electron at the origin, but also to the magnitude of this small admixture of states with an unpaired $6s$-electron, a fact that was even noted by Fermi and Segre[73]; there is no such strong dependence in the matrix elements of the weak interaction on this admixture. Similar results were obtained in Ref. 72 for thallium and lead.

TABLE II. Values of the A constant for the magnetic dipole hyper fine splitting (MHz) in bismuth.

	$^4S_{3/2}$	$^2D_{3/2}$	$^2D_{5/2}$	$^2P_{1/2}$	$^2P_{3/2}$
Experiment					
61		—1218			
68		—1230	2503	11310	
69	—447				
63		—1232 (6)		11272 (18)	
64	—456	—1217	2491		474
65	—446.937 (1)				
66					491.026 (1)
67		—1229 (60)		11269 (6)	
68		—1227.7 (2.1)	2501.8 (4.5)		
69			2503.3 (1.5)		
70		—1230.17 (15)		11268 (2)	
51			2502.86 (56)		
71			2503.8 (1.6)		
Calculation neglecting configuration mixing[72]	321	—770	2640	10200	785
Final theoretical result[72]	—448.5	—1070	2392	10610	474

The results of calculations[52] of quadrupole and magnetic octupole HF constants for levels of the $6p^3$ configuration in bismuth displayed in Tables III and IV also agree well with experiments. In contrast to magnetic dipole constants, these constants depend very weakly on admixtures of other configurations. Only the quadrupole constant B of the $D_{5/2}$ state, which remains a pure state in both the LS- and in the jj-schemes, is an exception. Since the hyperfine quadrupole interaction has a different sign for electrons and holes, in the case of a precisely half-filled shell, the constant B vanishes for a pure state. Indeed, this small constant differs from zero only due to the admixture of the $6p^2$ np configuration with $n \geq 7$, as well as due to the second order contribution from magnetic dipole HF interactions. For this reason, it is not calculated too reliably. The computed values of the remaining constants B remain adjustable parameters for the corresponding three experimental values, and in addition, the quadrupole moment of the Bi^{209} nucleus is a free parameter. Computed in this manner, it turns out to be equal to

$$Q(Bi^{209}) = -0.41 \text{ barns}. \tag{38}$$

This value of Q was then used for calculating $B(^2D_{5/2})$.

The magnetic octupole moment of the Bi^{209} nucleus

$$\Omega(Bi^{209}) = 0.56\frac{|e|}{2m_p} \text{ barns} \tag{39}$$

was found by a single parameter fit of the computed

TABLE III. Values of the constant B for the electric quadrupole hyperfine splitting (MHz) in bismuth.

	$^4S_{3/2}$	$^2D_{3/2}$	$^2D_{5/2}$	$^2P_{3/2}$
Experiment				
61		—23 (?)		
68		—657	306	
62	—303			
63		—600 (60)		
64	—288	—681 *)	387	1145
65	—304.654 (2)			
66				978.569 (9)
67		—678 (60)		
68		—630 (15)	60 (120)	
69			—90 (60)	
70		—652.5 (3.0)		
51			14 (11)	
71			2 (23)	
Theory[52]	—314	—647	8.5 (7.0)	961

*Taken from ref. 70.

TABLE IV. Values of the constant C for magnetic octupole hyperfine splitting (MHz) in bismuth.

	$^4S_{3/2}$	$^2D_{3/2}$	$^2D_{5/2}$	$^2P_{3/2}$
Experiment [65] [66]	0.0165 (1)			0.0207 (5)
Theory[52]	0.0170	−0.0124	−0.0419	0.0205

values of the constants C to the two available experimental numbers.

The values of the multipole moments of the bismuth nucleus presented above, (38) and (39), agree with those indicated in Ref. 66, but obtained using a smaller number of adjustable parameters.

It should be emphasized that these checks, with the help of the analysis of the constants A, B, and C, do not duplicate, but rather supplement, each other, since the matrix elements of the magnetic dipole and electric quadrupole HF interaction depend differently on the upper and lower components of the Dirac wave functions of the external electrons. Further, the same product of Dirac radial wave functions in the magnetic dipole and octupole matrix elements is multiplied by different negative powers of r (we refer everywhere to relativistic calculations).

Thus, the HFS analysis shows that the potential (36) with the parameters (37) describes well the behavior of the wave function of the $6p$-electron at small distances. The precision with which the matrix elements of the weak interaction are calculated, in any case, is not nearly so small as the HFS constants. And not only because these matrix elements are much more sensitive to configuration mixing than the constants A. The point is that the weak interaction, in contrast to the hyperfine interaction, is proportional not to r^{-n}, but $\delta(\mathbf{r})$. For this reason, it is completely determined by the behavior of the wave function near the nucleus, where this function is well-known to be hydrogen-like to within the normalization. And, in heavy atoms, where the motion of the external electron is primarily quasiclassical, this normalizing factor is expressed in terms of the spectrum of the electron,[73] which in its turn is reproduced well by the effective potential used.

Of course, these considerations, generally speaking, are not applicable to light atoms, where the motion of the external electron is far from quasiclassical. For this reason, the low precision of the calculation of the matrix elements of weak interaction in helium, discovered in Ref. 116, despite the opinion of the authors of that article, can by no means cast doubt on the precision of calculations based on the effective potential in heavy atoms. We also note that the effective potential in heavy atoms correctly reproduces in the Thomas-Fermi approximation the field created by the internal electrons. Calculations in helium with the help of such a potential[116] are, first of all, not justified physically. And finally, in contrast to the calculation in Ref. 116, the calculations[36] in heavy atoms are quite stable relative to variations of the potential parameters.

TABLE V. Lifetimes of excited states in bismuth, ns.

	$6p^27s^4P_{1/2}$	$6p^26d^2D_{3/2}$	$6p^27s^4P_{1/2}$	$6p^27s^2P_{3/2}$	$6p^26d^2D_{5/2}$	$6p^27s^4P_{5/2}$
Experiment [77]	5.9 (2)					
[78]		28 (2)	7 (2)		1.0—2.5	4.90 (25)
[79]	4.7 (1.0)	27 (3)	4.3 (4)	4.8 (4)	3.8 (1.0)	5.5 (5)
[80]	4.3 (2)	27.6 (5)	7.0 (2)	5.3 (2)	3.4 (2)	5.1 (3)
[81]				5.18 (20)		
Theory[76]	5.05	27.2	4.75	4.5	2.95	4.8

Let us now proceed to a discussion of the amplitudes of the $E1$-transitions $6p$–ns, $n \geq 7$. In thallium, the experimental values[74,75] of the radial integrals for the $E1$-amplitudes were used directly for $6p$–$7s$, $8s$, and $9s$ transitions. The calculation using the effective potential (36) gives results somewhat greater than these amplitudes. For this reason, at higher excitations of the $6p$-electron, for which the oscillator strengths are not known experimentally, correction factors, obtained by extrapolation of the corresponding corrections for lower excitations, were introduced into the calculation of the radial integrals. However, since the contribution of the high excitations of $6p$-electrons to circular polarization of radiation is in itself not large, the correction mentioned above to these amplitudes is generally not very significant.

In lead and bismuth, the values of the radial integrals for the $E1$-transitions $6p$–ns, $n \geq 7$, were obtained from the results of a numerical calculation by introducing the same correction factors that were necessary for the corresponding transitions in thallium. These values of the radial integrals were checked[76] by calculating the lifetimes of the excited states of lead and bismuth. The results of this check for bismuth are displayed in Table V. We note that, as the analysis carried out in Ref. 76 showed, mixing between levels belonging to the configurations $6p^27s$ and $6p^26d$ in bismuth is by no means always small. The reason for this lies in the fact that some of these levels are situated so close to each other that the spacing between them is comparable with the residual, nonspherically symmetrical, interaction between electrons. It is easy to show, however, that the contribution of this mixing to parity nonconservation effects is determined by the ratio of the residual interaction not to the spacing between the levels that are mixed as a result of it, but to the much greater spacing between levels with opposite parity. For this reason, this mixing has a small effect on the magnitude of the circular polarization, changing it by not more than 5–7%. A similar conclusion was reached in Ref. 38.

Let us go on to excitations of the type $6s6p^{k+1}$. The behavior of the wave function of the $6s$-electron as $r \to 0$ can be computed quite well with the help of the effective potential used above. This is supported by the fact that in thallium, where one of the levels with the excited $6s$-electron $6s6p^2$ lies in the discrete spectrum, such a calculation of the HF structure of this level agrees well with experimental values.[82]

As far as the amplitude of the E1-transition 6s–6p

is concerned, its value in thallium, as follows from an analysis of the experimental data,[83,84] is much less than that which is obtained by calculations with the effective potential or by using the Hartree-Fock method. In lead and bismuth, this quantity is not known experimentally. The correctness of the numerical values of these quantities for lead and bismuth, as adopted in Ref. 36, is supported by the fact that these numbers serve as a direct extrapolation of the corresponding values obtained from an analysis[78] of the experimental data for neighboring elements: gold, mercury, and thallium,[83-87] as shown in Table VI. We note that the near equality of the values as shown in the table indicates the smallness of the admixture of the $6p^{k+2}$ configurations to $6s^26p^6$,[76] since in gold such mixing is undoubtedly absent. Estimates show that taking admixtures of the $6p^5$ configuration to $6s^26p^3$ in bismuth into account can change the computed magnitude of the circular polarization by several percent. The same conclusion was reached in Ref. 38.

And, finally, in order to calculate the contribution of $6s6p^{k+1}$ excitations to circular polarization, it is necessary to know the energy of the $6s$-electron. In thallium and lead, this energy can be extracted from the experimental spectral data, and in addition, this quantity turns out to be noticeably less than that found by computations using the effective potential or the Hartree-Fock method. In this situation, the authors of Ref. 36 used the experimental values of the energies of the $6s$-electron in thallium and lead, while in bismuth, they used a value that was obtained by extrapolation of the data for thallium and lead and that is also much less than the computed value. It is the magnitude of the contribution of the $6s6p^{k+1}$ contribution that was the basic reason for the disagreement between the results of the calculations performed by different groups as mentioned above. According to recent theoretical studies[38-40] in Seattle and Oxford, account of the polarization of closed shells decreases the computed value of the amplitude of the $E1$-transition $6s-6p$ significantly. The results of these new calculations are close to those obtained in Novosibirsk (see Table I).

Numerical calculations show that the correction to the degree of circular polarization, arising from the excitation of electrons from inner shells that are deeper than the $6s^2$ shell, are of the order of 3–4%. The conclusion that this contribution is small is also reached in Ref. 88. An estimate of this effect, given in Refs. 89 and 90, according to which its magnitude amounts to ~20%, is too high, at least, if we are talking about a correction to our calculation. The point is that by far the largest part of the contribution mentioned arises in Refs. 89 and 90 due to the residual spherically symmetrical interaction between electrons, which does not have to be taken into account in the same manner, since it is already included in the initial spherically symmetrical effective potential when this potential is chosen correctly. Another serious argument that supports this fact is the good agreement of the computed values of the tensor polarizability of the $6p_{1/2}$ level in thallium with the experimental values (see below).

We note that an important factor in the reliability of the calculation is the fact that for each of the $M1$-transitions examined in thallium, lead, and bismuth, the contribution of all excitations to the circular polarization have the same sign. Moreover, the contributions of the excitations $6p-7s$ and $6s-6p$, for which we have direct or at least indirect experimental information, dominate the answer. However, as noted in Ref. 88, if the $E1$-transition operators are not expressed in the r-form, $-e\mathbf{r}$, as done in Refs. 36–40, but in the v-form, $(ie/\omega)\boldsymbol{\alpha}$, then not only do the different contributions to the circular polarization turn out to have opposite signs, but the contribution of the transition $6p-ns$ with $n>7$ becomes very important, especially for the continuous spectrum, which has been studied experimentally much less well. For this reason, it is clear that the calculation of circular polarization using the v-form of the $E1$-transition operator is unstable relative to comparatively small errors in the magnitude of separate contributions. The large deviation of the results of such a calculation from the result in Refs. 36–40, as discovered in Ref. 91, serves only as an additional illustration of this instability (see the analysis in Ref. 88) and by no means does it cast any doubt on the results obtained in Refs. 36–40 with the use of the r-form.

An important check on the precision of the Novosibirsk calculations is the good agreement with the experimental values of the polarizability of lead[76] and the tensor polarizability of the $6p_{1/2}$- and $6p_{3/2}$-states of thallium,[92] based on the same approach. They are presented in Table VII. Especially revealing is the agreement in the tensor polarizability of the $6p_{1/2}$-level of thallium, where the effect arises only for $F=1$ due to the HF interaction and for this reason the behavior of the wave function is checked simultaneously at large and small distances.

The results, enumerated here, of the numerous checks of the computational technique by comparing the computed atomic properties with the experimental data provide the basis for considering the precision of the Novosibirsk predictions,[36,37] presented in Table I, for

TABLE VI. Radial integrals.

$$\rho(6s, 6p) = \frac{1}{a}\int_0^\infty dr\, r^3 R_{6s}(r) R_{6p}(r)$$

	Au	Hg	Tl	Pb	Bi
Z	79	80	81	82	83
ρ	−2.2 [a]	−1.9 [a]	−1.75 [a]	−1.6 [b]	−1.5 [b]

a) Experimental values; b) values adopted in ref. 36.

TABLE VII. Polarizability of lead and tensor polarizability of thallium.

	$\alpha_{Pb}/\lambda=633$ nm, a^3	$\alpha^{ten}_{Tl}(6p_{1/2})$, Hz/(V/cm²)	$\alpha^{ten}_{Tl}(6p_{3/2})$, Hz/(V/cm²)
Experiment	49.4 (8) [93]	$-3.74(9)\cdot10^{-8}$ [94]	$-6.04(8)\cdot10^{-8}$ [94]
Theory	52 [76]	$-3.7\,10^{-8}$ [92]	$-5.85\,10^{-8}$ [92]

the circular polarization of radiation in normal $M1$-transitions in thallium, lead, and bismuth, in any case, as not worse than 15–20%. Despite widespread opinion, this precision is comparable with the precision of calculations of parity nonconservation effects in deep inelastic scattering of electrons, which, according to Refs. 95 and 96, constitutes 5–10%.

The numbers presented in Table I for Novosibirsk differ from those obtained in Ref. 36 (if trivial modifications relating to the fact that the value 0.25 is used for $\sin^2\theta$ instead of 0.32 are neglected) only by several percent due to some theoretical refinement of the $M1$-amplitudes, carried out in Ref. 37. First of all, in calculating these amplitudes, the difference between the radial wave functions of the $6p_{1/2}$- and $6p_{3/2}$-electrons was now taken into account in all three elements. Second, in lead and bismuth, the coefficients in the expansion of the wave functions in terms of pure jj-states were chosen so as to reproduce best the experimental values of the g-factors of the $6p^2$ states with total angular momentum $J=2$ in lead[97,98] and the $6p^3$ states with $J=\frac{3}{2}$ in bismuth.[62,66] The advantage of this computational method lies in the fact that, as is well-known,[17,18,99,100] the g-factor, just as the $M1$-amplitudes, is much less sensitive to admixtures of other configurations than the position of the energy levels, the fitting of which leads to the standard intermediate coupling expansion coefficients mentioned above. The values of the reduced amplitudes of the $M1$-transitions in bismuth, obtained in this manner,[37] are presented in Table VIII. The errors indicated in the Table correspond to a scatter of the intermediate coupling coefficients for which the computed values of the g-factors differ from the experimental values by not more than 10^{-3}. The best precision in fitting the g-factors by varying the coefficients is meaningless since relativistic corrections and configuration mixing effects together with spin orbital interaction make a contribution of approximately the same size, $10^{-4}-10^{-3}$, to these coefficients. Unfortunately, two independent g-factors of states with $J=\frac{3}{2}$ do not permit finding uniquely three parameters with which the expansion coefficients can be determined. For this reason, the errors in the amplitudes $(1-2)\cdot 10^{-2}$ noticeably exceed the allowed deviation from the experimental values of the g-factors, 10^{-3}. There is every basis to believe that the values of the $M1$-amplitudes found in this manner coincide with the true values within the indicated errors. For comparison, the same Table displays the results of a calculation based on the standard values of the intermediate coupling coefficients[66] and not taking into account the difference of the $6p_{1/2}$ and $6p_{3/2}$ radial wave functions; it is these quantities that were used in previous calculations of P-odd effects in bismuth.[36,38-40]

TABLE VIII. Reduced $M1$-amplitudes $A(M1)/\mu_B$ for bismuth.

λ, nm	876	648	462	301
New values[37]	−1.67 (2)	−0.55 (1)	−0.60 (1)	0.22 (2)
Standard values[66]	−1.72	−0.58	−0.62	0.19

Further increase in the precision of the calculation in bismuth could be achieved by a more detailed, and not average, analysis of the excitations involving the $6s6p^4$ configuration. Unfortunately, the experimental data, with the help of which this could be done comparatively easily, are not currently available.[4)] From estimates obtained for the transition $^4S_{3/2}-^2D_{5/2}$, the most probable result of such a refinement is an increase in the computed magnitude of the effect by several percent. It is also quite feasible to take into account quantitatively the mixing of the states $6p^27s$ and $6p^26d$. Apparently, the effect of mixing of $6s^26p^3$ with $6p^5$ can also be analyzed quantitatively. These theoretical investigations are currently being carried out in Novosibirsk.

6. PROSPECTS FOR FURTHER INVESTIGATION OF THE STRUCTURE OF WEAK INTERACTIONS IN EXPERIMENTS WITH HEAVY ATOMS

The investigation of weak interactions in atomic experiments is only beginning. Only the total "weak charge" of the bismuth nucleus has been measured. However, it is extremely important to know the "weak changes" of the neutron and proton separately. Unfortunately, due to the lack of precision in atomic calculations it is difficult to expect that such information can be extracted by comparing P-odd effects in atoms of different heavy elements even with high experimental precision; we note that in making the transition from cesium to bismuth the constant q [see (3)] changes by only several percent. It would probably be more promising from this point of view, to compare the optical activity of the vapors of different isotopes of thallium and lead (unfortunately, bismuth does not have stable isotopes). And although the expected magnitude of this difference is small, $\sim 1/Z$, this experiment will no longer be considered as fantastic.

At the present time, experiments involving the effects of parity nonconservation in heavy atoms that depend on the spin of the nucleus are completely feasible. As a result of this dependence, there is a small difference in the optical activity for different HF components of transitions in bismuth.[101] The effect arises due to the interaction of the weak vector current of the electrons with the axial current of the nucleons. With the appropriate dimensionless constant $\varkappa_2 \sim 1$ [see (1)], its relative magnitude attains several percent.[101] However, in the Weinberg–Salam model with $\sin^2\theta$ close to $\frac{1}{4}$, the constants $\varkappa_{2p,n}$ are very small. At the same time, in the effect being discussed, the contribution of the $\varkappa_3$ term to the Hamiltonian (1) increased proportionately[102] which could be referred to as the neutral weak magnetism. This contribution is enhanced by the presence of the spatial derivative and in bismuth constitutes about 20%

[4)] In this connection, we would like to draw the attention of experimentalists to the study of autoionized states, involving the configuration $6s6p^3$ in lead and $6s6p^4$ in bismuth.

of the contribution of the interaction with $\varkappa_2$ for $\sin^2\theta = 0.23$.

The contribution of radiative corrections to eN-scattering to this effect is somewhat smaller than that of neutral magnetism.[103-105]

The contribution of nuclear forces that do not conserve parity, and thanks to which the P-odd electromagnetic interaction of electrons with the nucleus arises,[106] are entirely comparable with the interaction depending on $\varkappa_2$ (see also Ref. 107). Thus, atomic experiments can provide valuable information concerning the violation of parity conservation in the nucleus.

It turns out that the effects of weak interaction of the electron and the nuclear spin are enhanced in molecules consisting of two different atoms, due to the very small distance between the levels with opposite parity.[108-110] Experiments searching for optical activity of heavy diatomic molecules, suggested in Ref. 109, are very promising.

These investigations will provide detailed information concerning the structure of parity-nonconserving weak interaction of electrons and nucleons, the existence of which is now reliably established.

The authors are sincerely grateful to A. I. Vaĭnshteĭn, V. N. Novikov, Yu.I. Skovpen', O. P. Suchkov, and V. V. Flambaum for numerous useful discussions, and to I. I. Gurevich, L. B. Okun', V. A. Sidorov, and A. N. Skrinskiĭ for their active interest in this work. The authors acknowledge with deep gratitude the support that A. M. Budker has given to this research.

[1]L. M. Barkov and M. S. Zolotorev, Pis'ma Zh. Éksp. Teor. Fiz. 27, 379 (1978) [JETP Lett. 27, 357 (1978)].
[2]L. M. Barkov and M. S. Zolotorev, Pis'ma Zh. Éksp. Teor. Fiz. 28, 544 (1978) [JETP Lett. 28, 3503 (1978)]; also, in Neutrinos-78, Conference Proceedings. Ed. by E. C. Fowler, Purdue University, 1978, p. 423.
[3]S. Weinberg, Phys. Rev. Lett. 19, 1264 (1967); Phys. Rev. D 5, 1412 (1972).
[4]A. Salam in: Elementary Particle Physics, Ed. by N. Svartholm, Stockholm, 1968, p. 367.
[5]C. Prescott *et al.*, Phys. Rev. Lett. B 77, 347 (1978).
[6]A. N. Moskalev, R. M. Ryndin, and I. B. Khriplovich, Usp. Fiz. Nauk 118, 409 (1976) [Sov. Phys. Usp. 19, 220 (1976)].
[7]A. I. Vaĭnshteĭn and I. B. Khriplovich, Usp. Fiz. Nauk 112, 685 (1974) [Sov. Phys. Usp. 17, 263 (1974)].
[8]F. J. Hasert *et al.*, Phys. Lett. B 46, 121 (1973).
[9]F. J. Hasert *et al.*, Phys. Lett. B 46, 138 (1973).
[10]A. Benvenuti *et al.*, Phys. Rev. Lett. 32, 800 (1974).
[11]B. L. Ioffe, Usp. Fiz. Nauk 110, 357 (1973) [Sov. Phys. Usp. 16, 459 (1974)].
[12]Ya. B. Zel'dovich, Zh. Éksp. Teor. Fiz. 36, 964 (1959) [Sov. Phys. JETP 9, 682 (1959)].
[13]M. A. Bouchiat and C. Bouchiat, Phys. Lett. B 48, 111 (1974).
[14]Ya. B. Zel'dovich, Zh. Éksp. Teor. Fiz. 33, 1531 (1957) [Sov. Phys. JETP 6, 1184 (1958)].
[15]L. M. Barkov, I. B. Khriplovich, and M. S. Zolotorev, Comm. Atom. and Mol. Phys. 8, 79 (1979).
[16]L. D. Landau and E. M. Lifshitz, Kvantovaya mekhanika (Quantum Mechanics), Nauka, Moscow (1974), p. 309.
[17]M. A. Bouchiat and C. Bouchiat, J. de Phys. 35, 899 (1974).
[18]I. B. Khriplovich, Yad. Fiz. 21, 1046 (1975).
[19]I. B. Khriplovich, Pis'ma Zh. Éksp. Teor. Fiz. 20, 686 (1974) [JETP Lett. 20, 315 (1974)].
[20]P. G. H. Sandars in: Atomic Physics V Ed. by G. zu Putlitz, Plenum Press, New York, 1975, p. 71.
[21]D. C. Soreide and E. N. Fortson, Bull. Am. Phys. Soc. 20, 491 (1975).
[22]G. Karl, Can J. Phys. 54, 568 (1976).
[23]M. A. Bouchiat and L. Pottier, Phys. Lett. B 62, 327 (1976).
[24]S. Chu, E. D. Commins, and R. Conti, Phys. Lett. B 60, 96 (1977).
[25]R. Conti, P. Bucksbaum *et al.*, Phys. Rev. Lett. 42, 343 (1979).
[26]M. A. Bouchiat and L. Pottier, Lecture at the Intern. Workshop on Neutral Current Interactions in Atoms, Cargese, 1979.
[27]M. A. Bouchiat and C. Bouchiat, J. de Phys. 36, 493 (1975).
[28]C. E. Loving and P. G. H. Sandars, J. Phys. B 8, L336 (1975).
[29]O. P. Sushkov, V. V. Flambaum, and I. B. Khriplovich, Pis'ma Zh. Éksp. Teor. Fiz. 24, 502 (1976) [JETP Lett. 24, 461 (1976)].
[30]D. V. Neuffer and E. D. Cummins, Phys. Rev. A 16, 844 (1977).
[31]R. R. Lewis and W. L. Williams, Phys. Lett. B 59, 70 (1975).
[32]E. A. Hinds and V. W. Hughes, Phys. Lett. B 67, 487 (1977).
[33]R. R. Lewis, Invited Address at the IV Intern. Conf. on Hyperfine Interactions, Madison, Wisconsin, 1977.
[34]R. T. Robiscoe, Phys. Lett. B 71, 360 (1977); *ibid.* 73, 158 (1978).
[35]E. C. Adelberger and T. A. Trainor, Lecture at the Intern. Workshop on Neutral Current Interactions in Atoms, Cargese, 1979.
[36]V. N. Novikov, O. P. Sushkov, and I. B. Khriplovich, Zh. Éksp. Teor. Fiz. 71, 1665 (1976) [Sov. Phys. JETP 44, 872 (1976)].
[37]O. P. Sushkov, V. V. Flambaum, and I. B. Khriplovich, Lecture at the All-Union Conference on the Theory of Atoms and Molecules, Vil'nyus, 1979.
[38]E. M. Henley, M. J. Klapisch, and L. Wilets, Phys. Rev. Lett. 39, 994 (1977).
[39]M. J. Harris, C. E. Loving, and P. G. H. Sandars, J. Phys. B 11, L749 (1978).
[40]E. N. Fortson and R. Katz (to be published); cited in Neutrinos-78: Conf. Proceedings, Ed. by E. C. Fowler, Purdue University, 1978, p. 437.
[41]D. C. Soreide, D. E. Roberts, *et al.*, Phys. Rev. Lett. 36, 352 (1976).
[42]I. I. Sobel'man, Vestn. Akad. Nauk SSSR No. 5, 18 (1978).
[43]L. M. Barkov and M. S. Zolotorev in Neutrinos-77, Conf. Proc. II, [Russian translation], Nauka, Moscow (1978), p. 329.
[44]L. M. Barkov and M. S. Zolotorev, Kvant. Élektron. (Moscow) 5, 1737 (1978) [Sov. J. Quantum Electron. 8, 986 (1978)].
[45]L. M. Barkov, M. S. Zolotorev, V. M. Khorev, V. P. Cherepanov, and A. I. Shekhman, Preprint IYaF-79-50, Novosibirsk (1979).
[46]B. A. Baklakov, V. F. Veremeenko, M. M. Karliner, A. A. Litvinov, and S. P. Petrov, Preprint IYaF-74-70, Novosibirsk (1974).
[47]A. M. Batrakov and V. R. Kozak, Avtometriya No. 4, 59 (1978).
[48]S. Mrozowski, Phys. Rev. 62, 526 (1942); *ibid.* 69, 169 (1946).
[49]V. N. Novikov, O. P. Sushkov, and I. B. Khriplovich, Opt. Spektrosk. 43, 621 (1977); *ibid.* 45, 413 (1978) [Opt. Spectrosc. (USSR) 43, 370 (1978); *ibid.* 45, 236 (1978)].
[50]G. J. Roberts, P. E. G. Bairds, M. W. S. M. Brimicombe, P. G. H. Sandars, D. R. Selby, and D. N. J. Stacey, J. Phys. B 13, 1389 (1980).

[51]J. Dembczynski, B. Arcimovicz, and K. Wisniewski, J. Phys. B 10, 2951 (1977).
[52]Yu. I. Skovpen', Opt. Spektrosk. 49, (1980) [*sic*].
[53]L. M. Barkov and M. S. Zolotorev, Phys. Lett. B 85, 308 (1979).
[54]P. E. G. Baird, E. N. Fortson, *et. al*. Nature 264, 528 (1976).
[55]P. E. G. Baird, M. W. S. M. Brimicombe, R. G. Hunt, G. J. Roberts, P. G. H. Sandars, and D. N. Stacey, Phys. Rev. Lett. 39, 798 (1977).
[56]L. L. Lewis, J. H. Hollister, D. C. Soreide, E. G. Lindahl, and E. N. Fortson, Phys. Rev. Lett. 39, 795 (1977).
[57]E. N. Fortson in Neutrinos–78, Conf. Proc. Ed. by E. C. Fowler, Purdue University (1978), p. 417.
[58]P. E. G. Baird, Lecture at the Intern. Workshop on Neutral Current Interactions in Atoms, Cargese, 1979; P. G. H. Sandars, private communication, June 1980.
[59]L. L. Lewis, Lecture at the Intern. Workshop on Neutral Current Interactions in Atoms, Cargese, 1979.
[60]A. E. Green, D. L. Sellin, and A. S. Zachor, Phys. Rev. 184, 1 (1969).
[61]H. Schüller, and T. Schmidt, Z. Phys. Bd. 99, S. 717 (1936).
[62]R. S. Title and K. F. Smith, Phil. Mag. 5, 1281 (1960).
[63]L. O. Dickie and F. M. Kelly, Canad. J. Phys. 45, 2249 (1967).
[64]J. Heldt, J. Opt. Soc. Am. 58, 1516 (1968).
[65]R. J. Hull and G. O. Brink, Phys. Rev. A 1, 685 (1970).
[66]D. A. Landman and A. Lurio, Phys. Rev. A 1, 1330 (1970).
[67]S. George and R. Klingberg, J. Opt. Soc. Am. 60, 869 (1970).
[68]R. Winkler, O. Gursch, and D. Skrok, in Proc. 5th Conf. of the European Group for Atomic Spectroscopy, Lund, Abstract No. 46.
[69]G. Muller, Doctoral Dissertation, Technishe Universität, West Berlin, 1974.
[70]J. Dembczynski and M. Frackowiak, Acta Phys. Pol. A 48, 139 (1975).
[71]L. M. Barkov and M. S. Zolotorev, Lecture at the Intern. Workshop on Neutral Current Interactions in Atoms, Cargese, 1979.
[72]O. P. Sushkov, V. V. Flambaum, and I. B. Khriplovich, Opt. Spektrosk. 44, 3 (1978) [Opt. Spectrosc. (USSR) 44, 2 (1978)].
[73]E. Fermi and E. Segré, Mem. Acad. D'Italia 4, 131 (1933); also E. Fermi, Scientific Works [Russian translation], Moscow (1972), Vol. 1, p. 485.
[74]N. P. Penkin and L. N. Shabanov, Opt. Spektrosk. 14, 167 (1963) [Opt. Spectrosc. (USSR) 14, 87 (1963)].
[75]A. Gallagher and A. Lurio, Phys. Rev. A 136, 87 (1964).
[76]V. V. Flambaum and O. P. Sushkov, J. Quant. Spectros. Radiat. Transfer 20, 569 (1978).
[77]P. T. Cunningham and J. K. Link, J. Opt. Soc. Am. 62, 1118 (1972).
[78]S. Svanberg, Phys. Scripta 5, 73 (1972).
[79]T. Anderson, O. H. Madsen, and G. Sorenson, J. Opt. Soc. Am. 62, 1118 (1972).
[80]A. L. Osherovich and V. V. Tezikov, Opt. Spektrosk. 44, 219 (1978) [Opt. Spectrosc. (USSR) 44, 128 (1978)].
[81]O. Poulsen and J. L. Hall, Phys. Rev. A 19, 1089 (1978).
[82]W. R. S. Garton, E. M. Reeves, and F. S. Tomkins, Proc. Roy. Soc. (London) A 341, 163 (1974).
[83]V. K. Prokof'ev and A. N. Filippov, Zh. Éksp. Teor. Fiz. 4, 31 (1934).
[84]G. V. Marr, Proc. Roy. Soc. (London) A 224, 83 (1954); G. V. Marr and R. Heppinstall, Proc. Phys. Soc. London 87, 2943 (1966).
[85]N. P. Penkin and I. Yu. Yu. Slavenas, Opt. Spektrosk. 15, 9 (1963) [Opt. Spectrosc. (USSR) 15, 3 (1963)].
[86]A. Lurio, Phys. Rev. A 140, 1505 (1965).
[87]J. N. Dodd, W. J. Sandle, and O. M. Williams, J. Phys. B 3, 3256 (1970).
[88]P. G. H. Sandars, Phys. Scripta 21, 284 (1980).
[89]D. B. Saakyan, I. I. Sobel'man, and E. A. Yukov, Pis'ma Zh. Éksp. Teor. Fiz. 29, 258 (1979) [JETP Lett. 29, 232 (1979)].
[90]D. A. Kirzhnitz and Yu. E. Lozobik, Pis'ma Zh. Éksp. Teor. Fiz. 29, 317 (1979) [JETP Lett. 29, 285 (1978)].
[91]S. L. Carter and H. P. Kelly, Phys. Rev. Lett. 42, 966 (1979).
[92]Yu. I. Skovpen' and V. V. Flambaum, Opt. Spektrosk. 45, 851 (1978) [Optic and Spectrosc. 45, 731 (1978)].
[93]A. A. Grebenyuk, Opt. Spektrosk. 49, 840 (1980) [Opt. Spectrosc. (USSR) 49, 459 (1980)].
[94]H. Gould, Phys. Rev. A 14, 922 (1976).
[95]L. Wolfenstein, Nucl. Phys. B 146, 477 (1978).
[96]E. Derman, Phys. Rev. D 19, 1333 (1979).
[97]H. M. Gibbs, Phys. Rev. D 5, 2408 (1972).
[98]A. Lurio and D. A. Landman, J. Opt. Soc. Am. 60, 759 (1970).
[99]M. Phillips, Phys. Rev. 88, 202 (1952).
[100]O. P. Sushkov, V. V. Flambaum, and I. B. Khriplovich, Zh. Éksp. Teor. Fiz. 75, 75 (1978) [Sov. Phys. JETP 48, 37 (1978)]; Phys. Lett. A 67, 177 (1978).
[101]V. N. Novikov, O. P. Sushkov, V. V. Flambaum, and I. B. Khriplovich, Zh. Éksp. Teor. Fiz. 73, 802 (1977) [Sov. Phys. JETP 46, 420 (1977)].
[102]I. B. Khriplovich, Yad. Fiz. 31, 1529 (1980) [Sov. J. Nucl. Phys. 31, 793 (1980)].
[103]W. J. Marciano and A. I. Sana, Phys. Rev. D 17, 3055 (1978).
[104]R. N. Mohapatra and G. Senjanovic, Phys. Rev. D 19, 2165 (1979).
[105]Yu. I. Skovpen' and O. P. Sushkov, Yad. Fiz. (1980) [Sov. J. Nucl. Phys. (in press)].
[106]V. V. Flambaum and I. B. Khriplovich, Zh. Éksp. Teor. Fiz. 79, 1656 (1980)[Sov. Phys. JETP 52, 835 (1980)].
[107]E. M. Henley, W. Y. P. Hwang, and G. N. Epstein, Preprint RLO–1388–797.
[108]L. N. Labzovskiĭ, Zh. Éksp. Teor. Fiz. 75, 856 (1978) [Sov. Phys. JETP 548, 434 (1978)].
[109]O. P. Sushkov and V. V. Flambaum, Zh. Éksp. Teor. Fiz. 75, 1208 (1978) [Sov. Phys. JETP 48, 608 (1978)].
[110]V. G. Gorshkov, L. N. Labzovskiĭ, and A. N. Moskalev, Zh. Éksp. Teor. Fiz. 76, 414 (1979) [Sov. Phys. JETP 49, 209 (1979)].
[111]R. Hultgren *et al*., Selected Values of Thermodynamic Properties of Elements, American Society of Metals, Washington, 1973.
[112]C. Prescott *et al*., Phys. Lett. B 84, 524 (1979).
[113]E. N. Fortson, private communication, June 1980.
[114]Yu. V. Bogdavnov, I. I. Sobel'man, V. N. Sorokin, and I. I. Struk, Pis'ma Zh. Éksp. Teor. Fiz. 31, 234 (1980) [JETP Lett. 31, 214 (1980)].
[115]Yu. V. Bogdanov, I. I. Sobel'man, V. N. Sorokin, and I. I. Struk, Pis'ma Zh. Éksp. Teor. Fiz. 31, 556 (1980) [JETP Lett. 31, 522 (1980)].
[116]J. Hiller and J. Sucher *et al*., Phys. Rev. A 21, 1082 (1980).

Translated by M. E. Alferieff
Edited by R. T. Beyer